Road Materials and Pavement Design

ISSN: (Print) (Online) Journal homepage: https://www.tandfonline.com/loi/trmp20

A brief review of sealants for cement concrete pavement joints and cracks

Lu Lu, Deying Zhao, Jizhou Fan & Guoqiang Li

To cite this article: Lu Lu, Deying Zhao, Jizhou Fan & Guoqiang Li (2022) A brief review of sealants for cement concrete pavement joints and cracks, Road Materials and Pavement Design, 23:7, 1467-1491, DOI: 10.1080/14680629.2021.1898452

To link to this article: https://doi.org/10.1080/14680629.2021.1898452

ROAD MATERIALS AND PAVEMENT DESIGN
2022, VOL. 23, NO. 7, 1467–1491
https://doi.org/10.1080/14680629.2021.1898452

Taylor & Francis
Taylor & Francis Group

A brief review of sealants for cement concrete pavement joints and cracks

Lu Lu[a], Deying Zhao[a], Jizhou Fan[a] and Guoqiang Li[b]

[a]Louisiana Multi-Functional-Materials Group LLC, Baton Rouge, LA, USA; [b]Department of Mechanical & Industrial Engineering, Louisiana State University, Baton Rouge, LA, USA

ABSTRACT

Pavement, as an important transportation infrastructure, plays an essential role in modern society. Joints and cracks, which are either designed for or created by internal and external means, must be filled in with proper sealant to stop penetration of water into the surface layer and layers beneath; otherwise, they usually lead to severer premature structural failure. In this paper, we briefly reviewed the various types of sealants available for cement concrete pavement, their performance, and their selection and evaluation methods. In particular, we discussed some new developments in sealant research, that is, using shape memory polymers as sealants. We concluded the brief review with some future perspectives.

ARTICLE HISTORY
Received 14 September 2020
Accepted 28 February 2021

KEYWORDS
Sealant; pavement; joint; crack; shape memory polymer; smart sealant

1. Introduction

Joints are designed and intentionally created in cement concrete pavement so that random premature cracks due to temperature or moisture changes can be minimised, controlled and managed. Therefore, although not universally accepted to seal all cracks/joints, sealing active joints/cracks (joints/cracks widen/narrow daily or seasonably), is widely acknowledged as a means to extend the pavement service life. The purposes of sealing joints/cracks are (1) to prevent obstruction of incompressible materials into the reservoir; (2) to reduce the amount of water infiltrating the pavement structure; and (3) to decrease the potential for dowel bar corrosion by reducing entrance of de-icing chemicals. A wide variety of caulking and sealant materials with different properties are available today for sealing cement concrete pavement joints and cracks. They are based on different reagents and/or formulations, meeting governmental and/or ASTM standards for consumers and contractors.

Agencies building and maintaining concrete pavements, in particular airport runways, require sealing joints for new pavements in the United States (Odum-Ewuakye & Attoh-Okine, 2006). Studies have demonstrated the effectiveness of crack sealing practice on the nation's highways (Al-Mansour et al., 1994; Chong, 1990; Eaton & Ashcraft, 1992; Smith & Romine, 1993). Not only sealing new joints but also resealing concrete pavement joints has been beneficial. The average frequency of joint resealing is approximately once every five years (Peterson, 1982). However, crack sealing to pavements with extensive cracking can pose a skid resistance hazard (Fried et al., 2019). Lee et. al. discussed several causes for sealant premature failure and one important reason was that the *in situ* joint openings were larger than AASHTO predictions (Lee & Stoffels, 2003). They suggested using the Lee–Stoffels model to predict the magnitudes of joint opening with its probabilities.

Most joint failures within concrete pavement are caused by failures at the joint rather than the pavement slabs. The failures include adhesive failure and cohesive failure in general, and faulting, pumping,

CONTACT Guoqiang Li lguoqi1@lsu.edu

blowups, spalling, corner breaks and mid-panel cracking in particular. Sealant damage mechanism has been studied by finite element analysis, thus appropriate frequency for maintenance, or joint resealing, can be determined (Herabat & Kerdput, 2006).

Over the years, a couple of excellent reviews have been published on pavement sealants (Eaton & Ashcraft, 1992; Odum-Ewuakye & Attoh-Okine, 2006). Although sealant has been used for over a century, it is still an active research area, partly because of the need for new sealants, and partly because of the advancement in new sealant materials, for example, shape memory polymer-based sealant. The purpose of this review is to briefly summarise the sealant research over the years, with a focus on new development. The paper is organised as follows. We will first review the typical failure modes of sealant. We will then discuss sealant evaluation approaches and sealant selection criteria. Following these discussions, we will introduce the types of sealants available in the marketplace and in the literature. In particular, we will introduce some new developments in sealant research based on smart materials. Finally, we will conclude with future perspectives. It is noted that, while cracks in both cement concrete pavement and asphalt concrete pavement need sealing, this review will focus on cement concrete pavement. However, because crack sealing in both cement concrete pavement and asphalt concrete pavement shares similar sealant and similar installation protocols, we will occasionally mention crack sealing in asphalt concrete pavement in this review.

2. Sealants failure

Sealant failure can be broadly divided into two categories: adhesive failure and cohesive failure. Adhesive failure is the loss of bond between the sealant and concrete walls, while cohesive failure is the breakage in the sealant body. Adhesion failure is the most common cause of sealant failure, and it could start as early as after the first winter. For example, in Texas, crack sealant failures are particularly severe within the first three years of application or service life. The viscoelastic characteristics at low temperatures can play a critical role in preventing adhesion failure. Two types of hot-poured sealants and two-types of silicone sealants were selected for evaluation of the viscoelastic model and stress relaxation at low temperature (Li et al., 2017b). Based on the test results, the stress relaxation of hot-poured sealants is better than silicone sealants and expected to perform better in extremely cold climates. Several other tests for hot-poured bituminous crack sealants were also conducted to measure the ability of the material to resist cohesive and adhesive failures (Al-Qadi & Fini, 2011; Al-Qadi et al., 2007b). The weak boundary layer theory was used to evaluate the crack sealant adhesion failure under complex ambient service conditions (Cao et al., 2019). Texas Transportation Institute also developed a new laboratory evaluation method for the adhesive performance of crack sealants to ensure the proper selection of sealants for a given project (Hu et al., 2011). A low-temperature tensile tester was developed to evaluate the cohesive property of crack sealants (Xue et al., 2018). Methods were developed by Guo et al. to evaluate cohesion and adhesion of hot-poured crack sealant and the test results showed that the cohesion was sensitive to temperature variation but the adhesive forces were not (Guo et al., 2017). An adhesion test based on the modification of AASHTO TP 89 was developed to characterise the adhesion performance of sealants and claimed to have improved repeatability and accuracy (Sawalha et al., 2017).

Twelve bituminous crack sealants were installed and evaluated over 4 years in an urban setting with -40°C to $+40$°C temperature range and the researchers investigated the rout size on performance, failure trends and overall performance in comparison with standardised test results (Masson et al., 1999). Masson and Lacasse also investigated the effect of hot-air lance on crack sealant adhesion and concluded that the bituminous crack sealant and dry asphalt concrete adhesion and failure mechanism are governed by the sealant source, the type of aggregate in the asphalt concrete mix, and the heat treatment on the rout before pouring the sealant (Masson & Lacasse, 1999). Overheating can cause a 50% reduction in adhesion strength and lead to premature failure, so the lance should be operated at reduced temperatures. Wilde et.al. investigated the effect of crack sealant material and reservoir geometry on surface roughness of bituminous overlays and found out that cooler pavement surface

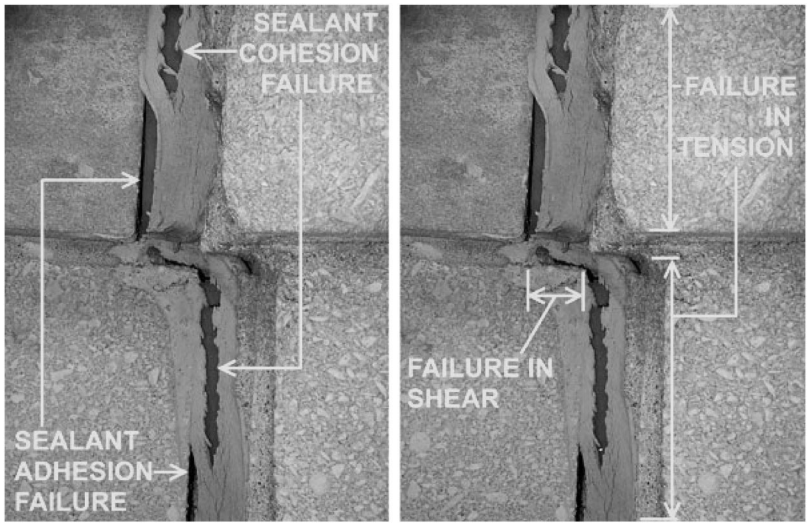

Figure 1. Sealant failure demonstration (with permission by Vina Trade Synergy Co., Ltd.) (Why Sealant Joints Fail: Avoiding Sealant Application Failures, 2018).

temperatures, no overband, hot-poured crumb rubber and hot-poured elastic sealants provide the best resistance to the formation of bumps in overlays (Wilde & Johnson, 2009). Induction heating technology was introduced by Partl et. al. in 2018 to improve the compaction of asphalt joints by adding iron particles into the asphalt mixture. The results showed that high temperature during compaction of the joint leads to a better overall performance of the pavement (Bueno et al., 2020).

Figure 1 shows typical adhesive and cohesive failure modes in the sealant (Why Sealant Joints Fail: Avoiding Sealant Application Failures, 2018). From Figure 1, it is clear that the failure is caused by two types of stress: tensile stress, which primarily causes joint widening due to temperature drops, and shear stress, which is mainly caused by traffic load. The sealant within the joint reservoir is in a complex stress condition. Once the tensile stress or shear stress is higher than the interfacial bonding strength between the sealant and concrete wall, adhesive failure occurs. On the other hand, once the tensile or shear stress is higher than the tensile or shear strength of the sealant itself, cohesive failure cannot be avoided. Figure 2 shows more failure modes of hot-poured bituminous sealant and silicone sealant in concrete pavements. Table 1 gives a detailed summary of the sealant failure mode and description for two types of sealants: field-molded sealants and preformed compression seals.

3. Sealant evaluation

Researchers have developed/proposed a series of test methods to evaluate sealant performance in field applications. The sealant performance at low temperature is the key factor limiting the development of crack sealing and filling of pavements (Li et al., 2009). Hu et. al. designed an overlay tester to conduct fatigue tests for sealants at low temperatures for 2000 cycles (Hu et al., 2011). Soliman and Shalaby used a dynamic shear rheometer and bending beam rheometer to evaluate joint and crack sealants performance in cold climates (Soliman et al., 2008). Later, they used glass transition temperature and stiffness at low temperatures to evaluate sealant performance (Soliman & Shalaby, 2009). They indicated that these two indexes were well correlated and proposed that the sealant glass transition temperature should be lower than the service temperature to maintain good performance. Rotational viscosity, penetration, softening point, ductility, and bond tests (ASTM D5329-07) were usually used to evaluate crack sealants. The method/index of principal component analysis was used to evaluate the performance of sealants and fillers for cracks in asphalt concrete pavements (Li et al.,

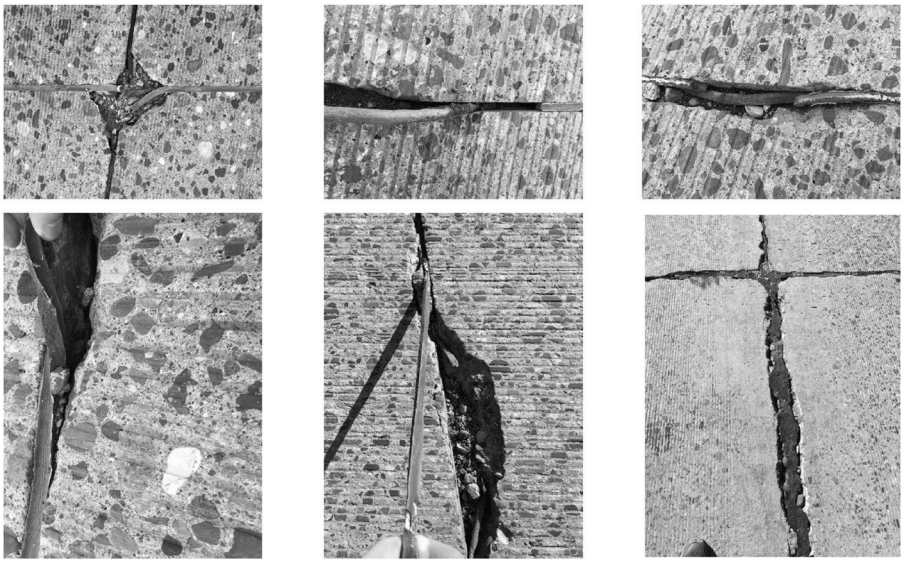

Figure 2. Typical failure modes of sealant in cement concrete pavements (photos taken by authors).

Table 1. Joint sealant failure mode and description (modified based on ref 1) (Odum-Ewuakye & Attoh-Okine, 2006).

Failure mode	Description
Field-molded sealants	
Partial depth adhesion loss	Sealant-joint separation only at one or both edges
Partial depth spalling	Slab cracking only at one or both edges within 2 feet
Partial depth cohesion loss	Sealant splitting due to over elongation but not extending vertically through the entire depth
Stone intrusion	Stones (diameter $>$ 0.25 inch) embedment into the sealant which cannot be easily removed
Preformed compression seals	
Partial depth adhesion loss	Sealant-joint separation only at one or both edges
Partial depth spalling	Slab cracking only at one or both edges within 2 feet
Stone intrusion	Stones (diameter $>$ 0.25 inch) embedment into the sealant
Surface extrusion	Sealant expansion above pavement surface due to twisting or high placement
Full-depth adhesion loss	Sealant separation from one or both edges of the joint
Full-depth spalling	Slab cracking from one or both edges within 2 feet, but vertically extending through the sealant
Full-depth cohesion loss	Sealant splitting vertically through entire depth
Sunken seal	Complete sealant separation from both edges and sunken into the joint
Twisted/rolled seal	Sealant twisted/turned in the joint and sealant surface not even
Compression set	Sealant structure losing ability to apply outward pressure
Gap	Joint width over the expansion limit of compression seal

2017a). Bending beam rheometer specimen was used to evaluate the low-temperature performance of bituminous crack sealants (Al-Qadi et al., 2005). Loannides et al. tracked the joint sealant performance at the Ohio Route 50 site for 3 years, involving 10 different sealant compounds (4 silicone, 2 hot-applied, and 4 compression seals) and 4 unsealed sections (Ioannides et al., 2004). The results showed that compression seals generally outperformed the other sealants and the crew experience in sealant installation is a critical factor. For hot-applied sealant for asphalt pavement, the viscosity evaluation index was also developed to test the viscosity of the sealants and determine the pouring temperature (Li et al., 2015a). The short-term and long-term field ageing effects of hot-poured crack sealants through a differential ageing testing was conducted by Ozer et al (2015). For low temperature performance evaluation, ASTM D 5329 has been used. Figure 3(a) shows a schematic of the dimension of a specimen per ASTM D5329-16 standard for bond testing between the sealant and concrete

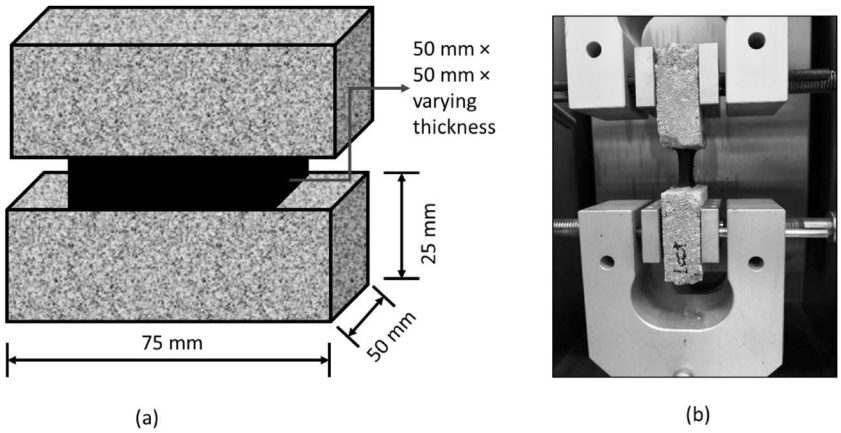

Figure 3. Example of bond test between the sealant and concrete wall per ASTM D 5329–16 standard. (a) A schematic of the dimensions of a test specimen; (b) A specimen under testing by the authors (Note: slightly modified to fit for the clamps of the MTS machine).

block, and Figure 3(b) shows such a specimen under testing by the authors. A modified direct tensile tester method was developed to characterise the low-temperature performance of the hot-poured crack sealant (Al-Qadi et al., 2007b). Linear viscoelastic modelling was conducted to understand the behaviour of hot-poured bituminous-based crack sealants at low service temperatures and to predict both thermal and traffic loading *in situ* (Al-Qadi et al., 2010). A laboratory test using Taber Abraser was used to rapidly assess the tracking resistance of bituminous crack sealant (Masson et al., 2007). Li et al. developed an adhesive strength test method to determine the adhesive strength of self-levelling and non-self-levelling silicone sealants between concrete pavement joints with proper test conditions (Li et al., 2014a; Petersen et al., 1998). Rogers et al. proposed a simple test method to simulate the movement of a typical transverse contraction joint used in joining concrete pavement sections constructed without dowel bars (Rogers et al., 1999a). The test apparatus can consider the effects of temperature, joint size, and pavement deflection on the performance of the sealant (Rogers et al., 1999a). Al-Qadi et al. proposed a crack sealant adhesion direct tensile (CSADT) test procedure. It uses a direct tensile tester with modifications to the end pieces and the specimen holder. In this test procedure, the sealant is confined between two aluminium pieces, which will move apart at 0.05 min until failure occurs. The failure load and the displacement at failure are recorded and then used to assess the sealant's adhesion capability. It was found that the repeatability of the suggested procedure was acceptable with an average coefficient of variation of 10.9% (Al-Qadi & Fini, 2011). Li et al. developed a new device, which was called the Creep Testing Apparatus (CRETA), for use in determining the viscoelastic properties of joint sealant. The test can be conducted considering various environmental conditions such as temperature, moisture and freeze–thaw (Li et al., 2012). Yun et al. proposed a device to test the slip-down failure of various preformed joint sealants (PJS) (Yun et al., 2011). Through the parameter resistant stiffness, which is determined by dividing the peak force by the displacement, they can correlate the slip-down distress and the joint width (Li et al., 2014b).

The key parameters for evaluating sealants are listed below:

- Elasticity: ability to return to the original shape and size after being deformed (stretched or compressed); most sealants depend on the ability to deform elastically to survive the harsh stress condition in the reservoir;
- Modulus: change in internal stress while being stretched and compressed over a range of temperatures; low modulus is desirable, particularly in cold weather; sealants with glass transition temperature lower than that of the working temperature ensure better low-temperature performance;

- Adhesion: ability to adhere to concrete surface both initially and long-term; good adhesion is the key for sealant to serve;
- Cohesion: the ability to resist tearing from tensile and shear stress; with soft sealant or high strength sealant or both, the stress in the sealant can be significantly reduced, and cohesive failure can be largely avoided;
- Compatibility: sealants with a certain chemical bond with concrete ensure good adhesion; good adhesion is an indication of compatibility;
- Weatherability: ability to resist deterioration is essential when the sealant is exposed to harsh environments such as saltwater, chemicals (e.g. anti-freezing agent), oil, and ultraviolet radiation.

4. Sealant selection

The ideal characteristics of sealants include: (1) providing a barrier in the joint/crack to minimise water penetration; (2) resilient enough to prevent debris from becoming retained in the joint/crack reservoir; (3) remaining flexible in various temperature regimes to accommodate for the expansion and contraction of the concrete slabs and (4) not softening in hot weather and not hardening in cold weather.

When selecting a sealant, the first thing is to investigate the condition and requirements for the actual application, such as the substrate type, the exposed weather conditions and the expected joint movement. The current specification system for selecting crack sealants is found in ASTM D6690, which focuses on using tests such as softening point and cone penetration (Ozer et al., 2014). Researchers validated the low-temperature selection thresholds for selecting hot-poured crack sealants (Ozer et al., 2014; Yang et al., 2010). They used nine hot-poured crack sealants installed in four test sites experiencing low temperatures for two consecutive years. Results showed a good correlation between low-temperature performance grade sealant thresholds and field performance. Li et al. thought the softening point test and the flow test, two existing methods for evaluating the high-temperature performance of hot-applied sealant, could not accurately reflect the adhesion performance of the sealant at high temperatures (Li et al., 2014b). They modified the adhesion test for PAST (pressure-sensitive adhesive tape) and believed the modified version is efficient in distinguishing the high-temperature adhesion performances of different sealants and can be used as a standard method for evaluating such performances (Li et al., 2014b). To select the best sealant for Utah, Biel et al. compared polyvinylchloride-coal tar, rubberised asphalt and silicone. However, it was difficult to choose the best type of sealant with a significant level of confidence. Silicone has been performing well and resealing of the joints after 10 years was recommended (Biel & Lee, 1997).

Rogers et al. proposed a three-step protocol for selecting sealant: (Rogers et al., 1999a; Rogers et al., 1999b) (1) use ASTM C794 adhesion-in-peel test to assess concrete/sealant adhesion; (2) use dynamic mechanical analysis to evaluate sealant flexibility and determine the glass transition temperature and(3) use shear fatigue test to analyze sealant performance under severe pavement deflection and various environmental conditions. Afterwards, the authors used the protocol to select/evaluate the adhesive strength, viscoelastic properties, and shear fatigue behaviour of two polyurethane joint sealants for use in undoweled concrete highway joints, and claimed that the correlation was conclusive (Rogers et al., 1999a). Masson et al. proposed to use physico-chemical methods to predict the short- and mid-term performance of sealant mixtures (Masson et al., 2002). One-year field performance of the sealants correlated well with viscometry and microscopy; while the mid-term performance had a reasonable correlation with the glass transition temperature.

Crack sealing is not a perfect means of preventive maintenance since premature sealant failure is common (Evers, 1983; Ward, 1993) in cold urban conditions, extensive failure is often evident within a few years of service. Therefore, more in-depth studies are still needed for sealant design and selection. In particular, how to correlate the lab-scale test results to real-world sealant performance remains a challenge.

There are several factors influencing sealant performance, and thus careful consideration of these factors would help sealant selection:

- Joint size (clearly, expansion joint needs more ductile sealant than contraction joint);
- Joint movement (for active joint, sealant is needed and must be carefully design; for freezing joint, sealant is generally not needed);
- Adhesion between sealant and joint (as one of the two major failure modes, adhesion between the sealant stripe and concrete wall is critical for success; development of chemical bond usually leads to better adhesion than physical interaction such as friction.)
- Sealant reservoir shape (shape factor has been a widely studied topic. Finite element modelling is a strong tool to evaluate the effect of shape factor on the stress in the sealant. For contraction joint, shape factor 1.0 is recommended);
- Sealant properties (The sealant performance depends on the sealant properties; elasticity, viscoelasticity, stiffness, glass transition temperature, and weatherability all determine the performance of the sealant);
- Voids under joint (for some cut through joints such as expansion joints, proper support to the sealant stripe from the bottom is critical to avoid slip-down failure; sand, bulse wood, laminate, etc., have been used to provide support at the bottom of the sealant);
- Quality of workmanship/inspection (reservoir cleaning, accurate reservoir dimension, surface roughness of the concrete wall, fully curing of the sealant and adhesive before opening to traffic, etc., are some of the factors that affect the sealant performance);
- Type and condition of pavement, including base course, subbase course, and subgrade (different base, subbase, subgrade, and concrete slab strength, stiffness, moisture content, and aging, affect the deflection of the concrete slabs under thermal and traffic loading, and thus the affect the tensile and shear strain in the sealant. These factors must be taken into account when selecting the sealant and designing the shape factor of the reservoir);
- Environmental factors (When selecting sealant materials, temperature, moisture, ultraviolet irradiation, and chemical attacks, must be considered. For example, in cold region, only ASTM Type IV bituminous sealant may be used);
- Traffic loading (traffic loading directly affects the stress in the sealant, and thus the performance of the sealant. Traffic loading such as equivalent single axle load (ESAL), channelisation, etc., must be considered when selecting sealant).

5. Types of sealants

Sealants can be classified by their state at the time they are installed into the joint (field-moulded or preformed); by the application procedure used to install the sealant (hot-applied, cold-applied, or compression seal); by the base component used to formulate the sealant (bitumen, coal-tar, polysulphide, polychloroprene, polyurethane, etc.); or by a characteristic that the material exhibits after installation (jet-fuel-resistant, heat-resistant, etc.).

Slurries of mud and clay were used as sealants in the very early days, which lacked flexibility and could not adjust to thermal expansion/contraction. Their weatherability was not good and had to be re-patched continuously. 'Caulk' is defined as a substance placed inside a joint to create a barrier to prevent the passage of air, heat, or water; while 'sealant' is defined as a material not only serving as 'caulk' but also being able to extend and compress without losing its sealing effectiveness (Foster, 1987). Therefore, we use the term sealant instead of caulk in this review.

5.1. Asphalt based sealant

Hot-poured rubberised bituminous compounds were the most popular type of sealant used since the early 1940s. Today, hot-poured rubberised bituminous sealants are still the most widely used materials

for joint and crack sealing due to the ease in installation and low cost. However, the sealant would be dissolved when subjected to fuel spillage in airfield parking aprons. In the mid-1950s, researchers were developing jet-fuel-resistant sealants.

Polymer/rubber modified bituminous sealant can degrade when heated to excessive temperatures and for extended periods (Linde & Johansson, 1992). Application temperature and heating time of the hot-poured bituminous sealant should be closely monitored so sealant degradation during crack sealing of pavement can be controlled (Masson et al., 1998). Masson et al. discussed the temperature control of hot-poured sealants during the sealing of pavement cracks and suggested the next generation kettles which allow for variable stirring speeds and be equipped with a digital gauge and automated temperature control so that a temperature feed-back loop will allow for automatic reading and readjustment of heating (Masson et al., 2005). To prevent degradation, sealants should be heated for less than 1 h at 170°C or use the lower end of the temperature range recommended by the manufacturer (Masson, 1997).

Coal-tar-based pavement sealants were identified as a major source of polycyclic aromatic hydrocarbons (PAH) in large parts of the U.S. (Christen et al., 2005; Mahler et al., 2005; Pavlowsky, 2013). Later on, researches have shown that coal-tar sealants would contribute PAH to various environmental compartments and the chemicals would generate potential risks to ecological communities (Bommarito et al., 2010a; Bommarito et al., 2010b; Bryer et al., 2010; Scoggins et al., 2007) and human health (Mahler et al., 2012; Williams et al., 2012; Williams et al., 2013). Metre et al. proved in 2014 that the PAH concentration in lake sediment declined following the ban on coal-tar-based pavement sealants in Austin, Texas (Van Metre & Mahler, 2014). PAH volatilisation following the application of coal-tar-based pavement sealant was measured and results suggested that PAH emissions from coal-tar-based sealcoat applications each year ($\sim$1000 mg) are larger than annual vehicle emissions of PAHs for the Unites States (Van Metre et al., 2012).

5.2. Polymeric sealants

In addition to bitumen or coal-tar based sealants, polymeric sealants have played a major role over the years. The earliest polymeric sealants were triglyceride esters of long-chain fatty acids. They were considered as low-performance sealants and showed little or no chemical curing after application. They were inexpensive, had little flexibility, and tended to crack when they were subjected to moderate joint movement. Solvent-based acrylics and butyl sealants are considered medium performance sealants. Butyl rubber is prepared by the polymerisation of isobutylene. Butyl sealants are relatively low in price and adhere to a wide range of substrates. Solvent-based butyl sealant shows joint shrinkage due to solvent loss and sealant stringiness during application.

Acrylic polymers are prepared by polymerising acrylic acid monomer $H_2C = CHCO_2H$ and its derivatives. The acrylic acid monomer can be converted into methyl acrylate or replacing the α-hydrogen with an alkyl group. The sealant properties can be tuned based on the monomers and polymerisation conditions. Outdoor sealing applications are suggested for acrylics due to the strong odour. It takes several months for a complete cure. Acrylics can adhere to a wide variety of substrates. However, shrinkage due to solvent evaporation and fair flexibility limited the application of acrylics sealants.

Water-based latex emulsion sealants are based on poly(vinyl acetate), poly(vinyl acrylics) or acrylic latexes. The advantages include the paintability, good UV stability, fast skin-over time, environmental acceptance and relatively low cost. However, due to the around 50% water content, shrinkage upon cure may happen and when stored at cold temperatures, sealants may be damaged from freezing. Hence, storing at warmer temperatures to avoid freezing or incorporating ethylene or propylene glycol into the formulation is necessary. The organism can grow in water, which subjects latex sealant to microbiological attack. Therefore, incorporating biocidal preservatives is a common practice. Acrylic latex has great weatherability and can be formulated into clear commercial products,

which cannot be achieved by polysulphide and polyurethane sealants. Acrylic latex sealants have passed high-performance specifications.

Polysulphides, polyurethanes and silicones are considered high-performance sealants. They are all chemically cured, which means curing takes place via chemical reaction after extrusion from the cartridge. There will be little or no shrinkage. They can cater for large joint movement.

Polysulphides are the first high-performance elastomeric sealants with excellent ductility and good water and solvent resistance. However, the nasty smell makes polysulphides not desired for indoor applications. Furthermore, weak packaging stability and long-term storage capability are the obvious disadvantages of polysulphide sealants.

Polyurethane (PU) has little odour. It can be cured by moisture in the air when reacting with an excess of diisocyanate. PU adheres to the widest range of substrates and has good toughness and abrasion resistance. However, PU has limited packaging stability, similar to polysulphide sealants, and poor UV stability. Therefore, incorporating UV stabilisers (Kiliaris et al., 2009) or having a layer of paint over the applied joint can be useful.

A two-component polyurethane modified with hydroxyl-terminated polydimethylsiloxane joint sealant was developed and its cohesion strength after hot pressing and hard drawing was higher than conventional PU and tar-based PU joint sealant (Xu et al., 2011a). An interpenetrating polymer network prepared with polyurethane and epoxy resin shows better damping properties and mechanical/thermal properties (Li & Mao, 1996; Liu et al., 2013; Wu et al., 2015; Zhang & Hourston, 1998). A system composed of epoxy acrylate, PU, and methyl methacrylate was used for asphalt pavement crack repair (Yin et al., 2018).

Silicones are considered as the best overall sealant in the market now. Silicones are prepared with organosilanes. Its repeating unit contains a Si-O backbone and the properties are mainly influenced by the 'R' group on the Si atom and the crosslinking agent used to polymerise organosilanes. They have superior elasticity, relatively short curing time, good weatherability and packaging stability, excellent thermal stability, and fair adhesion to a wide range of substrates (Stögbauer & Wolf, 1991).

Some of the first reported use of silicone pavement joint sealants were in 1954 (Britton, 1965), when the New York State Department of Public Works began to investigate materials that could be used to seal the expansion and contraction joints in bridges. The installation mistakes the contractors made-produced low performance of silicone sealants. Silicone sealants began to become more popular in building sealant in the 1960s (Tock et al., 1987) and were reintroduced into the pavement sealant market in the 1970s. The first field trials of low modulus silicone highway joint sealant were applied in Georgia in 1977 (Zimmer et al., 1984). Then it quickly covered other climate regions in the U.S. A generic silicone sealant specification was finally realised in 1996.

An elastomeric silicone foam sealant was developed for sealing bridge expansion joints with small movement in bridge decks, which had lower stiffness, greater extensibility, and better bonding associated with the foam sealant compared to the solid (unfoamed) sealant (Malla et al., 2007). The glass transition temperature of the silicone is about −120°C, which means that silicone will not harden within its service temperature range when it is used as pavement joint sealant (Malla et al., 2011).

Silicones can be categorised by the crosslinking agents or by the byproducts generated upon curing. The most common byproduct is the acetoxy type. Acetic acid is giving off during sealant production with moisture in the air, which gives a strong odour. Other types of silicone sealants are based on alkoxy, aminoxy, oxime, etc. These silicone sealants have less harsh odour and better adhesion to concrete and metals such as brass and copper. Silicone sealant lacks good paintability.

When elastomers are exposed to sunlight, oxygen, moisture, ozone, elevated temperature, surface chemicals, etc., sealant damages can happen including cracking, peeling, chalking, colour change or even failure. Malla et al. conducted temperature aging, compression recovery, creep and weathering for a foam silicone sealant (Malla et al., 2011). This work is the first experimental description of the behaviour of silicon foam sealant under conditions in the northern part of the U.S. during winter. Failures such as fall-down, material failure, and adhesive problems due to repeated traffic loading and the

contractive/expansive issues of concrete slabs are common for silicone rubber sealants. Experimental and numerical evaluations on the shape factor (the ratio of joint depth to joint width) of silicone sealant for concrete pavements under vertical loading was investigated (Ryu et al., 2018). Based on the results from the finite-element modelling (FEM), the optimised shape factor is suggested as 1.0 for sealants with 6.0 and 8.0 mm joint widths.

Block copolymers are good candidates for sealants, such as styrene–butadiene–styrene (SBS), styrene–isoprene–styrene (SIS) and styrene–ethylene–butylene–styrene (SEBS). Incorporating proper UV absorbers into SEBS based sealants can achieve excellent UV resistance. When necessary, clear sealants with good weatherability can be formulated. However, flammable organic solvents have to be used in manufacturing the clear block copolymer sealants.

Hybrids or blends of the high-performance sealants have the potential to be used as pavement sealants. Hybrid sealants can take advantage of the strengths of two and eliminate the weakness of the individual component. Sealants derived from sily terminated polyether has improved weatherability over standard PU sealants, while eliminating the odour and nonpaintability issues acetoxy silicone sealants have. It can also adhere to different substrates, and with good abrasion resistance and extrudability from the cartridge at low temperatures.

Other polymeric sealants developed by researchers may be directly used or modified to serve in pavement joints and cracks, such as structural glazing silicone sealant (Rosendahl et al., 2019), high vacuum leak sealant made with anaerobic polymers (Kendall, 1982), polyurethane sealants containing rosin for disc regeneration (Carbonell-Blasco et al., 2013), alkoxysilane terminated polymers (Huber et al., 2016), phenol-formaldehyde resin-based adhesive (Kubit et al., 2018), aerospace sealants based on polythioether polymer (Clark & Cosman, 2003), polyethylene nanocomposite sealant (Zhang et al., 2009), photo-induced smart self-healing polyisobutylene based polymer for photovoltaics (Bag et al., 2016; Banerjee et al., 2015), etc.

Sealant performance depends not only on the sealant properties, but also on other factors, including installation and curing conditions. Table 2 summarises the advantages and disadvantages of different sealant materials.

5.3. Sealant additives

Plasticisers are often added to sealants to lower the modulus, improve the flexibility of the cured product, and improve the extrusion of the sealant from the cartridge. There are a very wide selection of additives and a suitable one should be picked out which can form a homogenous blend. Hard fillers can reinforce sealants and reduce costs. Particle size and particle size distribution affect the strength and modulus of the cured product. Calcium carbonates and aluminium silicates are common fillers for sealants. When white sealants are required, titanium oxide can be utilised. Ready availability and compatibility should be considered when selecting the appropriate fillers. For water-based latex sealant, stabilisers such as ethylene glycol and propylene glycol should be used to achieve storage stability. Surfactants can aid in the mixing process, lower sealant viscosity, improving extrudability, and 'wetting' the surface on which it is applied. UV is a destructive force that causes surface degradation, including surface cracking, chalking, discolouration, and loss in adhesion. Antioxidants, such as hindered phenols and UV absorbers, for example, hindered amines and substituted benzotriazoles, can be added to the sealant to increase UV stability. Mildewcides can improve mildew and fungus resistance. To improve adhesion with the substrate, coupling agents and adhesion promoters can be used. For example, silanes and organotitanates can improve sealant-substrate adhesion. Catalysts can improve the curing characteristics of the sealant. Curing is defined as the conversion from a liquid state into a fixed or hardened state by chemical action such as oxidation, vulcanisation, polymerisation, etc., or physical action, such as evaporation of a volatile constituent. The most commonly used catalysts are peroxide, tertiary amines, or compounds based on metals such as nickel and tin. The properties of sealants modified with different additives are related to the mixture performance (Liu et al., 2016).

Table 2. Advantages and disadvantages of sealant materials (modified based on Foster).(Foster, 1987)

Type	Advantages	Disadvantages
Oil-based	• Low cost • Easy tools needed	• Poor joint movement • Limited adhesion • Hardens or cracks upon aging
Solvent-based acrylics	• Wide adhesion range • Good UV stability	• Strong odour • Slow curing • Limited joint movement
Solvent-based butyls	• Low cost • Wide adhesion range	• Joint shrinkage • Containing flammable solvent • Stringy when applied
Latex-based	• Water cleanup • Fast skinning • Good packaging stability	• High shrinkage • Poor early water resistance • Hard to extrude at low temperatures
Latex-based acrylic latex	• Good joint movement • Wide adhesion range • Good UV stability	• Poor joint shrinkage • Freezes at low temperatures
Polysulphide	• Excellent joint movement • Wide adhesion range	• Strong odour • Limited UV stability • Limited packaging stability
Polyurethane	• Excellent joint movement • Good adhesion range • Good abrasion resistance	• Poor UV stability • Limited packaging stability • Slow curing for one-component systems
Block copolymer	• Excellent UV stability • Good joint movement	• High joint shrinkage • Containing flammable solvents
Silicone	• Superior UV stability • Great joint movement • Fast curing	• Strong odour • High cost • Poor adhesion to concrete • Non-paintable
Modified silicone	• Excellent joint movement • Great UV stability • Wide adhesion range • Good paintability • No odour	• Moderate cost • Limited adhesion

5.4. Sealant specifications

The first government specification in the USA for cold-applied sealant was SS-S-156 in 1952 (emulsion type). Specification SS-S-200 was for two-component, cold-applied sealant. It included both jet-fuel and flame-resistance tests. The majority of the sealants manufactured to meet SS-S-200 were formulated using polysulphide or polyurethane as the base component. The most commonly used cold-applied sealant today is the silicone (polydimethylsiloxane) based materials. With the wide applications of sealant in pavements, bridge decks, and buildings, ASTM has developed a series of specifications for testing, evaluating, and selecting sealants. Some typical ASTM standards are summarised in Table 3.

In Europe, the Rabe-Test, which is German Standard TL Fug-StB 01, was introduced in 2001 to evaluate sealant materials.

6. Smart sealants

The last several decades have witnessed remarkable advances in smart materials, which will be playing a significant role in areas of aerospace, automotive, civil, mechanical, medical, and communication engineering fields. Among the smart materials family, shape memory polymers (SMPs) are an important member. SMP is a polymer that when it is deformed to a temporary shape, the shape can be maintained for a long time after removal of the external load; the temporary shape, however, can

Table 3. General characteristics and typical uses for sealant materials (Lynch & Janssen, 1998).

Specification	General Characteristics	Typical Use
ASTM D 1190	Asphalt-based, hot-applied, elastic-type sealant containing ground rubber and/or polymeric materials and reinforcing fillers. A thermoplastic material supplied in solid form from the manufacturer and heated to a liquid for insertion into the joint	Sealing joints and cracks in asphalt concrete (AC) and Portland cement concrete (PCC) pavements. Not intended for use in areas where fuel spillage is expected.
ASTM D 2628	Polychloroprene-based, preformed compression seal consisting of web design.	Sealing joints in PCC pavement. Generally used in new construction or reconstruction instead of resealing applications. Typically not used to seal cracks.
ASTM D 3405	Asphalt-based, hot-applied sealant containing ground rubber, and/or plasticizers, and reinforcing fillers. A thermoplastic material supplied in solid form from the manufacture and heated to a liquid for insertion into the joint.	Sealing joints and cracks in AC and PCC pavements. Not intended for use in areas where fuel spillage is expected.
ASTM D 3406	Coal tar-based, hot-applied sealant containing plasticizers and fillers. The materials are supplied in either a solid form or a liquid form that is heated before insertion into the joint. Crosslinking occurs during the heating of the sealant.	Sealing joints and cracks in PCC pavements. The sealant should not be used in AC pavements due to a potential incompatibility problem between the coal tar material and AC pavement.
ASTM D 3569	Coal tar-based, hot-applied, jet-fuel-resistant (JFR) sealant containing polyvinylchloride (PVC), plasticizers, and fillers. The thermoset materials are supplied in either a solid or liquid form from the manufacture that is heated before insertion into the joint. Crosslinking occurs during the heating of the sealant.	Sealing joints and cracks in PCC pavements where fuel spillage is expected. The sealant should not be used in areas where concentrated aircraft exhaust is expected or to seal cracks in AC pavement.
ASTM D 5078	Asphalt-based, hot-applied, filler containing ground rubber and fillers. The materials are supplied in solid form.	Filling cracks in AC pavements. The material is not a sealant and should not be expected to perform in the same manner as a sealant. The material is not JFR.
ASTM D 5893	Silicone-based (polysiloxane), cold-applied, single component, chemically curing materials. The materials are supplied in liquid form.	Sealing joints and cracks in PCC pavements. Some formulations can be used to seal cracks in AC pavements. The material is not typically considered to be JFR.
FS SS-S-1401	Asphalt-based, hot-applied sealant containing ground rubber, plasticizers, and/or polymeric materials, and reinforcing fillers. This material is similar to ASTM 3405 and is supplied in solid form.	Sealing joints and cracks in AC and PCC pavements. Not intended for use in areas where fuel spillage is expected.
FS SS-S-1614	Coal tar-based, hot-applied sealant containing PVC, plasticizers, and fillers. This material is similar to ASTM D 3569 materials.	Sealing joints and cracks in PCC pavements where fuel spillage is expected. The sealant should not be used in AC pavements due to a potential incompatibility problem between the coal tar material and AC pavement.
FS SS-S-200	Cold-applied, two-component, JFR, and heat resistant sealants typically containing polysulphide, polyurethane, or modified coal tars as the base component. The materials are supplied in either hand mix or machine mix formulations.	Sealing joints and cracks in PCC pavements that are subjected to fuel spillage and concentrated aircraft exhaust.

return to its original shape under proper stimuli. Based on the functional groups and morphology of the SMPs, the stimuli can be heat, light, pH, moisture, etc. The process of deforming the polymer and fixing a temporary shape is also called programming. During programming, the SMP is usually deformed at a temperature above the transition temperature (glass transition temperature for amorphous polymers or melting temperature for semi-crystalline polymers), followed by cooling and load removal (hot programming) (Hager et al., 2015; Hu et al., 2012). However, deforming an SMP specimen

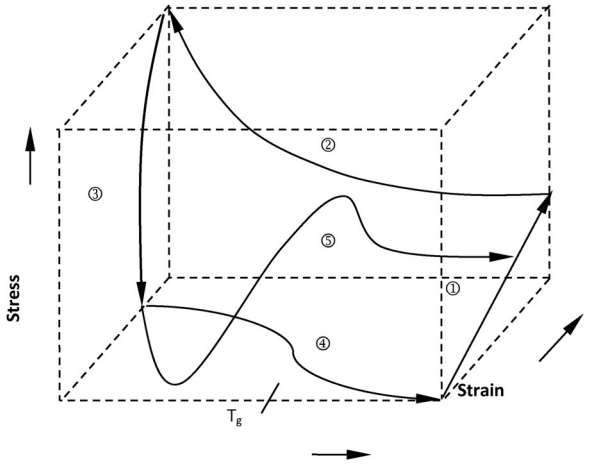

Figure 4. Schematic of classical hot tension programming (steps ①–③), free shape recovery (step ④), and fully constrained stress recovery (step ⑤) (Li, 2014) (Copyright of Wiley, reproduced with permission)

can also be done below the transition temperature (cold programming) (Li & Xu, 2011b) or within the transition zone (warm programming) (Li & Wang, 2016).

Next, we would like to discuss more details. In hot programming, the SMP is first heated up to above its transition temperature. For thermoset SMPs, the temperature is usually 20°C above their glass transition temperatures. The hot SMP is then deformed to a certain strain by external load such as tension, compression, bending, and twisting, or a combination thereof, and the deformation is maintained for a little while (usually several minutes) at this temperature. After that, the polymer is cooled down to below the transition temperature by either holding the stress constant (stress controlled) or holding the strain constant (strain controlled). Once the temperature reaches the designed low temperature, for example, 20°C below the glass transition temperature, the load is removed, usually accompanied by a small springback, completing the programming process. If the polymer is heated up above its transition temperature again, the polymer either restores its original shape (shape recovery), if no external constraint is applied, or releases a certain force (stress recovery), if an external constraint is applied. The programming process and the shape recovery process constitute a thermomechanical cycle. Figure 4 shows a typical thermomechanical cycle with hot tensile programming (steps 1–3), free shape recovery (step 4), or stress recovery (step 5) (Li, 2014). The shape memory effect (SME) is usually evaluated by shape fixity ratio and shape recovery ratio. The higher the ratios, the better the shape memory effect is. Usually, in terms of strain, the shape fixity ratio is defined as (Behl & Lendlein, 2007):

$$R_f(N) = \frac{\varepsilon_u(N)}{\varepsilon_m}, \tag{1}$$

where N is the number of thermomechanical cycles; R_f is the shape fixity ratio; ϵ_m is the pre-deformation strain and ϵ_u is the temporary strain fixed.

The residual strain after shape recovery, as compared to the pre-deformation strain, defines the shape recovery capability of the polymer, which is represented by the shape recovery ratio as follow (Behl & Lendlein, 2007):

$$R_r(N) = \frac{\varepsilon_m - \varepsilon_p(N)}{\varepsilon_m - \varepsilon_p(N-1)}, \tag{2}$$

where R_r is the shape recovery ratio, and ϵ_p is the permanent or residual strain. Again, N and ϵ_m are the same as in Equation (1).

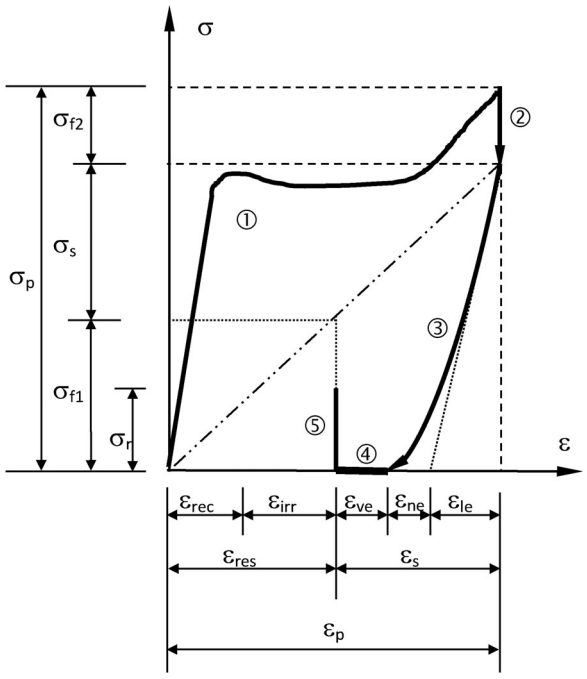

Figure 5. Schematic of stress-strain behavior of SMPs in the entire thermomechanical cycle by cold-compression programming (① – loading; ② – holding the strain constant for a while (stress relaxation); ③ – unloading; ④ – structural relaxation); and ⑤ fully constrained (stress recovery) (Li, 2014) (Copyright of Wiley, reproduced with permission).

For warm programming, the only difference from hot programming is that the deformation is applied within the glass transition zone. Because the stiffness of the polymer within the glass transition zone is higher than that in the rubbery state, the programming stress is higher than that in hot programming, in order to induce the same deformation. As compared to hot programming, warm programming needs less effort in heating and cooling, and may lead to slightly higher recovery stress (Li & Wang, 2016).

Because most structural polymers have a transition temperature above room temperature, cold programming suggests that the polymer can be deformed at room temperature, without the heating and cooling process. In cold programming, the polymer is deformed directly to a certain strain beyond yield strain, and the strain is maintained for a while to allow structural relaxation, followed by load removal and springback, completing the cold programming process (Li & Xu, 2011b). It has been proved that cold programming usually leads to higher recovery stress (Li & Wang, 2016; Li & Xu, 2011b). Figure 5 shows a schematic of the stress–strain behaviour a thermoset SMP under cold compression programming and constrained stress recovery. From Figure 5, the total programming stress, σ_p, can be decomposed into stress fixed, σ_f (σ_{f1} in Step 1 and σ_{f2} in Step 2), and stress corresponding to springback σ_s (linear elastic stress σ_{le}, nonlinear elastic stress σ_{ne}, and viscoelastic stress σ_{ve}), which is reversible and can be determined from the unloading stress–strain curve as shown in Figure 5. From this definition, it is clear that we define the fixed stress as subtracting the stress corresponding to springback from the peak applied stress. This makes sense because the fixed stress should be the portion of stress which causes fixed strain. Springback stress just causes elastic deformation, which is reversible. Therefore, removing springback stress from the programming stress is reasonable in order to determine the fixed stress. Of course, as shown in Figure 5, we have simplified the determination of the springback stress by an equivalent linear elastic relationship of the unloading stress–strain behavior (the dot-dot-dash line), just like a linear elastic spring does when the applied load is removed. More studies are needed to better represent the springback stress. Similarly, the total programming

strain, ϵ_p, can be divided into springback strain, ϵ_s, and residual visco-plasto-damage strain, ϵ_{res}. The springback strain ϵ_s is further decomposed into linear elastic strain, ϵ_{le}, nonlinear elastic strain, ϵ_{ne} and viscoelastic strain, ϵ_{ve}. It is noted that the linear and nonlinear elastic strains are independent of time during unloading process, while the viscoelastic strain is time-dependent after fully removal of the applied stress. It usually takes from minutes to hours to stabilise after the removal of the applied load. The residual visco-plasto-damage strain, ϵ_{res}, is further divided into irrecoverable strain, ϵ_{irr}, and recoverable strain, ϵ_{rec}. More detailed decomposition can further divide the irrecoverable strain into irreversible plastic strain and damage. Sometimes, we can also call the recoverable strain, which is the portion that can be recovered due to shape memory, as reversible plastic strain, meaning a type of plastic strain that can be recovered, in order to differentiate from the classical definition of plastic strain, which is permanent strain and cannot be recovered.

Based on Figure 5, the shape fixity ratio is re-defined as (Li, 2014; Li & Wang, 2016):

$$R_f = \frac{\varepsilon_{res}}{\varepsilon_p}, \tag{3}$$

The shape recovery ratio R_r is re-defined as the recovered strain over the fixed strain (Li, 2014; Li & Wang, 2016):

$$R_r = \frac{\varepsilon_{rec}}{\varepsilon_{res}}, \tag{4}$$

It is noted that this definition for shape recovery ratio is different from the definition by Behl and Lendlein (2007). In their definition, the shape recovery ratio for the first thermomechanical cycle is:

$$R_r = \frac{\varepsilon_p - \varepsilon_{irr}}{\varepsilon_p} = \frac{\varepsilon_s + \varepsilon_{rec}}{\varepsilon_s + \varepsilon_{res}}, \tag{5}$$

In other words, the shape recovery ratio is defined as the ratio of the recovered strain (springback strain and shape memory strain) over the programming strain. Obviously, if the springback strain (ϵ_s) is small, which is usually the case for hot programming, the two definitions yield similar results; if the springback strain is large, such as in cold programming, the two definitions yield considerably different results. Because springback does not represent shape memory, we advocate Equation (4).

The mechanisms for shape memory effects (SMEs) have been widely studied. One is entropy-based theory and the other is enthalpy-based theory. In entropy-based SMPs, programming reduces the conformational entropy by aligning the molecules or segments along the loading direction, and thus in the temporary or deformed shape, the SMPs are in a nonequilibrium state with reduced entropy. When the SMPs are heated up above their transition temperature, entropy increases automatically driven by thermodynamic forces, forcing the aligned molecules or segments to return to their original coiled configuration, and leading to shape recovery (Lendlein & Kelch, 2002). For SMPs with high steric hindrance in their molecular structures, the programming energy can also be stored in the form of enthalpy increase during deformation, through chemical bond length and bond angle change (Fan & Li, 2018; Wick et al., 2021; Yan & Li, 2020). When the SMPs are heated up, free volume increases, and coordinated segmental rotation becomes possible, until the stored energy is released, leading to shape recovery. Usually, SMPs based on enthalpy storage exhibit higher recovery stress (Li et al., 2018).

Because the basic requirement for sealant is that it behaves thermally opposite to the construction materials, that is, when the pavement contracts, the sealant expands, and when the pavement expands, the sealant contracts, Li's group at Louisiana State University proposed to use SMPs as potential sealants through proper programming. In 2011, Li and Xu investigated polystyrene-based shape memory and self-healing syntactic foam as sealants for expansion joints (Li & Xu, 2011a). In this idea, an SMP based syntactic foam is programmed in two directions: compression in horizontal or traffic direction, and tension in the vertical direction. In the summer, when the pavement temperature exceeds the glass transition temperature of the foam, shape recovery of the foam is triggered, leading to a contraction in the vertical direction, thereby avoiding the problem of sealant squeezing out of the

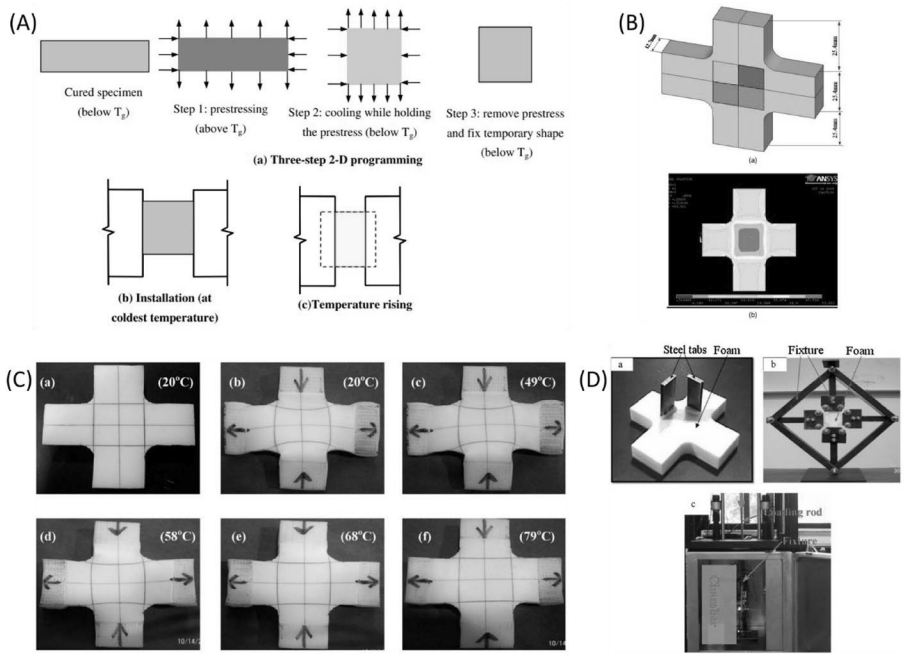

Figure 6. Polystyrene-based sealants designed and developed in the Li group (Li & Xu, 2011a; Xu & Li, 2011a). (A) Illustration of sealant programming, installation, and performance during temperature rising. (B) The biaxial specimen dimensions and von Mises stress distribution. (C) The original (a) and programmed (b) cruciform foam sealant specimen, along with the recovery process under various temperatures (c)–(f). (D) The programming setup and testing method of the cruciform foam specimen. (Copyright of ASCE: (A), (C), and (D), and Copyright of Elsevier: (B), with reproduced permissions).

reservoir. In the horizontal direction, the foam recovers and expands in the horizontal direction. At the same time, the neighbouring concrete slabs also expand. As a result, the foam will be further compressed in the horizontal direction, instead of expansion. This stored compression will be utilised in the winter. When the temperature drops in the winter, the highly compressed foam expands in the horizontal direction when the neighbouring concrete slabs contract or retreat. As a result, even in the winter, the foam remains in close contact with the concrete slabs, avoiding adhesive failure problem at low temperature. The idea is schematically shown in Figure 6(A) (Li & Xu, 2011a). This idea has been validated by both lab-scale experimentation and field-level installation. In lab-scale experimentation, the cyclic stress–strain behaviour of the polystyrene-based shape memory sealant was programmed by 2-D stress condition through a crossform device (Xu & Li, 2011a) see Figure 6(B) for the crossform specimen, Figure 6(D) for the test assembly and test apparatus, and Figure 6(C) for the two-directional programmed specimen in the recovery process from (b) at room temperature up to (f) at 79 ^{o}C, leading to complete shape recovery (the shape in (f) is fully returned to the original shape in (a)). The effect of ultraviolet radiation on the morphology and thermo-mechanical properties (Xu et al., 2011b) and durability under accelerated hydrolytic aging (Xu & Li, 2011b) of the shape memory polymer based syntactic foam sealant were investigated. The results show that the SMP based syntactic foam is durable.

Considering that in field-level applications, large SMP panels needs to be programmed (compression in horizontal or traffic direction and tension in the vertical direction) in order to solve the debonding problem at low temperature and sealant squeezing-out-of the reservoir problem in the summer, a two-stage hybrid 1D programming was conducted, which proved to be able to replace the one-stage 2D programming (Li et al., 2013). Figure 7 shows the stress–strain-time relationship of the sealant in the entire thermomechanical cycle (programming and free shape recovery) (Li et al., 2013). The behaviour of the SMP based syntactic foam under cyclic loading conditions was also investigated

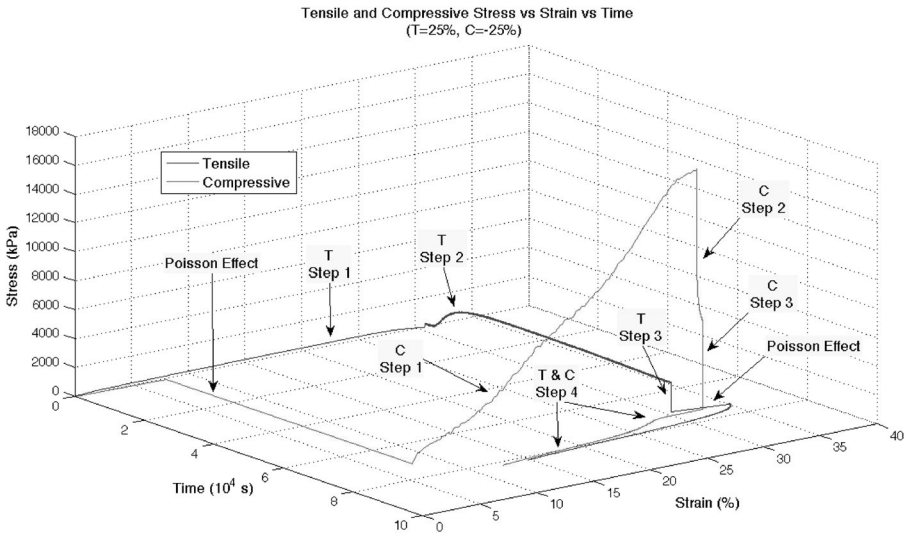

Figure 7. Full thermomechanical cycle in both tension and compression directions for a specimen programmed by 25% tensile strain at a temperature above the glass transition temperature, followed by 25% compression at a temperature below the glass transition temperature in the transverse direction, in terms of stress-strain-time scale (T represents tension, C stands for compression, and T&C represents coupled tension and compression) (Note: To have both tension and compression directions in the same quadrant, the compression stress and compression strain are also treated as positive) (Li et al., 2013). (Copyright of ASCE, reproduced with permission)

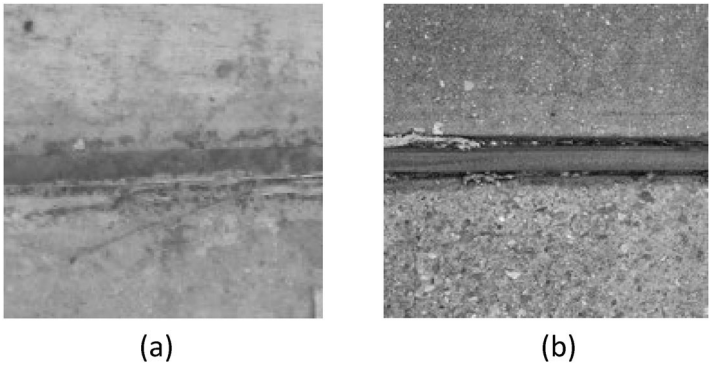

Figure 8. Shape memory PU sealant installed in a cement concrete pavement at Louisiana State University campus, which is a street with commuting buses. (a) Sealant after installation in January 2012, and (b) the same sealant in September 2020.(Photos took by the authors)

(Xu & Li, 2011a). In field level installations, Li's group selected two expansion joints in a cement concrete pavement at the Louisiana State University campus, which is a road for heavy bus traffic. They used the two-stage programming approach, and used shape memory polyurethane (PU) as sealant (Li et al., 2015b). The two stripes of sealant were installed in January 2012 (Li et al., 2015b). A silicone rubber-based adhesive was used to bond the programmed PU stripes to the concrete wall. After about nine years of service, the two joints are still in very good condition; see Figure 8. From Figure 8, one can see that, while the abrasion of the concrete slab is significant, the PU sealant stripe is in good condition. However, loss of adhesive is seen, suggesting that the abrasion resistance of the silicone-based adhesive is not as good as the PU sealant.

Shape memory PU has disadvantages include lower tensile and compressive strength, weaker thermal stability, and smaller shape recovery force (Meng & Hu, 2009; Xu et al., 2011a). The limitations can

be improved by adding fibres, particles, nanotubes, graphene, etc., as reinforcement (Chen et al., 2016; Haghayegh & Mir Mohamad Sadeghi, 2012; Jancar et al., 2010; Li et al., 2015b; Thakur & Karak, 2015; Zhang et al., 2016; Zohrevand et al., 2014). Shen et al. synthesised a TiO_2/PU sealant used for expansion joint after the two-stage biaxial programming. The shape memory transition temperature was in the range of 50–60°C (Shen et al., 2018b). Shen et al. also used epoxy to modify shape memory PU as a sealant, with improved tensile properties (Shen et al., 2018a).

Another recent development in smart sealant is to use two-way shape memory polymers (2W-SMPs) as sealants. As compared to the above SMPs, which is also called one-way SMPs, that is, new programming is required after each shape recovery event, 2W-SMPs can reversibly shift between the original and temporary shapes, without the need for subsequent programming (Lu & Li, 2016). This behaviour has been utilised to fabricate polymeric artificial muscle through twist insertion of precursor 2W-SMP fibres (Fan & Li, 2017; Yang et al., 2016; Yang & Li, 2016). For semi-crystalline 2W-SMPs, the driving force for the two-way shape memory effect (2W-SMEs) is due to rubber elasticity at temperatures above the crystallization temperature and melt/crystallization transition at temperatures below the crystallization temperautre (Yan et al., 2020). With a proper initial tensile programming, 2W-SMPs can behave thermally opposite to common physics, that is, expansion upon cooling and contraction upon heating. Because of this unique behaviour, Li proposed that 2W-SMPs can be used as sealants (Li, 2014; Li, 2020). Lu et al. have investigated two 2W-SMPs that have the potential to serve as sealants (Lu et al., 2018; Lu et al., 2017a). The advantage of using 2W-SMP as sealant as against 1W-SMP as sealant is that 2W-SMP sealant may not need programming before installation. The daily temperature drop in the field may provide the tensile stress necessary for tensile programming the 2W-SMP sealant. To prove this idea, Lu et al. simulated the daily temperature cycle without programming (Lu et al., 2018). With cooling, they gradually added tensile stress to the specimen, and with heating, they gradually removed the applied load. As shown in Figure 9, the temperature drop (blue line) induced a step increase in stress on the sealant (black line), and the strain reached $\sim$150%. Temperature increase led to the expansion of the concrete slab, and tensile stress on the sealant was gradually reduced, resulting in contraction of the sealant. At the completion of each cooling/heating cycle, the stress became zero and the strain also became zero. While the thermal cycle accompanied by loading and unloading cannot be directly regarded as 2W-SME, because loading will cause extension and unloading will cause shortening, it is believed that the deformation is primarily due to 2W-SME. This is because the large expansion under a small tensile stress (0.25 MPa) and a modulus of several hundreds of MPa at freezing temperature can only produce a tiny expansion strain, instead of the over 100% expansion shown in Figure 9. Therefore, it is believed that 2W-SMP has a good potential to be used as sealant.

7. Concluding remarks and future perspectives

Due to the large market needs and unsatisfactory performance of currently available sealants, research and development in the joint/crack sealant area should continue. In this paper, we briefly reviewed the existing sealant materials, from bituminous sealant, to polymeric sealant. Our focus is on introducing a new type of emerging research – using shape memory polymers (SMPs) or their composites as sealant. With their unique properties that meet the needs of sealant requirements, such as expansion upon cooling and contraction upon heating, SMPs have a good potential to be used as sealants.

In this paper, the basic ideas of using one-way shape memory polymer (1W-SMP) or two-way shape memory polymer (2W-SMP) as sealant are discussed, and some preliminary results are summarised. For 1W-SMPs, it is found that with a proper two-step programming (compression in horizontal direction and tension in vertical direction), they have a potential as a new type of smart sealant in concrete pavement joints and cracks, avoiding the problem of sealant squeezing out of the reservoir in the summer, and adhesive failure (debonding of the sealant from the concrete wall) in the winter. This concept has been proved preliminarily by both lab scale experimentation and field level installation.

We also reviewed another new concept – using 2W-SMPs as sealant. As compared to the 1W-SMP sealant, which needs two-step programming, and is a challenge in field-level applications, 2W-SMPs

do not need such programming. The natural temperature drop in the field can serve as the means of tensile programming. Preliminary lab-scale test results show that a semicrystalline 2W-SMP, which is a chemically crosslinked *cis* polybutadiene, has a potential to be used as a sealant, including in cold regions, due to its large expansion at freezing temperatures.

However, the existing studies on both 1W-SMPs and 2W-SMPs as sealant are still in their infant stage, more pavement performance-based studies are required such as viscoelasticity, adhesive failure, cohesive failure, fatigue, fuel resistance, flame retardancy, etc. In addition, how to design this type of sealant is largely unknown. Some design factors such as shape factor of the reservoir, strength, stiffness, toughness, compatibility, shape fixity ratio, shape recovery ratio, etc., of the sealant, need to be studied. Future studies should be towards finding appropriate adhesive to bond solid SMP stripes to concrete walls. Liquid version SMPs, either hot-pour or clod-pour, with curing *in-situ* capability should be more convenient, which also avoids the need for adhesive, and thus should be developed (Li, 2020). Furthermore, just like conventional sealants, testing and evaluation methods for smart sealants need to be developed. Simple lab scale testing methods that have a good correlation with field-level performance should be the research focus. Many studies have been conducted and test apparatus has been developed to evaluate the performance of existing sealants such as fatigue, adhesion, cohesion, tension, shear, creep, viscoelasticity, glass transition temperature, environmental attacks, effect of concrete moisture and aging, and slip-down failure (Ozer et al., 2015; Al-Qadi et al., 2007a; Al-Qadi et al., 2010; Masson et al., 2007; Petersen et al., 1998; Al-Qadi & Fini, 2011; Li et al., 2012; Yun et al., 2011; Ozer et al., 2014; Yang et al., 2010; Li et al., 2014a; Li et al., 2014b; Li et al., 2015a; Li et al., 2015b; Li et al., 2017a; Li et al., 2017b; Biel & Lee, 1997; Rogers et al., 1999a; Rogers et al., 1999b; Masson et al., 2002; Evers, 1983; Ward, 1993; Foster, 1987; Linde & Johansson, 1992; Masson et al., 1998; Masson et al., 2005). These previous studies are of great reference values for the smart sealant evaluation and design.

Finally, some other properties such as damage self-healing should be incorporated in the SMP based sealants. Some existing bituminous sealants have demonstrated such capability (Bueno et al., 2020; Tan et al., 2020). Many strategies have been proposed for healing polymers and polymer composites (Li, 2014). As for the self-healing of SMPs, there are primarily two strategies: one is the biomimetic close-then-heal (CTH) strategy by simulating the self-healing of human skin (Li & Nettles, 2010; Li & Uppu, 2010), and the other is shape memory assisted self-healing (SMASH) (Rodriguez et al., 2011). The CTH strategy aims at healing wide-opened cracks. In this strategy, a shape memory polymer matrix is first compression programmed before service. During service, assuming a macroscopic crack

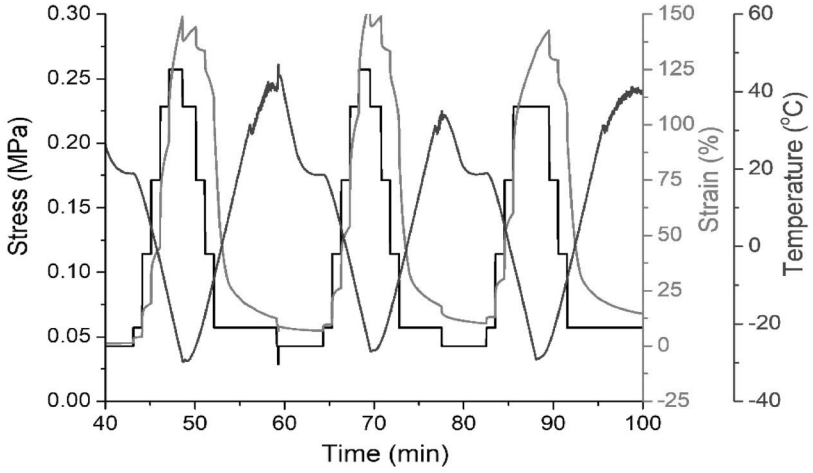

Figure 9. The 'real world simulation' for cured *cis* polybutadiene after installation. Simulation of the daily temperature cycle, accompanied by loading and unloading. The 2W-SME and loading/unloading effect may be coupled. (Open Access by Springer Nature, reproduced with permission) (Lu et al., 2018).

is created, the crack can be healed molecularly based on the CTH strategy. To heal the crack, the SMP or SMP based composite needs to be heated up to above its glass transition temperature, which leads to constrained shape recovery (expansion) of the SMP matrix. Due to the constraint by the boundary or surrounding cold materials, the growth in volume cannot occur; instead, the SMP matrix pushes to the open space inside (crack), leading to narrowing or closure of the wide-opened crack. Further heating can either lead to extrinsic molecular scale healing by embedded healing agent (John & Li, 2010; Li & John, 2008; Nji & Li, 2010a; Nji & Li, 2010b; Nji & Li, 2012) or lead to intrinsic molecular scale healing by the polymer itself such as shape memory vitrimer (Feng et al., 2019; Feng & Li, 2020; Li et al., 2018; Lu et al., 2016; Lu et al., 2017b). On the other hand, SMASH strategy does not conduct programming before service, or depends on the damage itself as *ad hoc* programming, and thus it can only bring narrow cracks to closure (Menon et al., 2019). Therefore, if the constraint surrounding the crack is high or if the shape recovery ratio is not 100%, SMASH strategy cannot bring wide-opened crack in touch. Hence, we expect that the CTH strategy can be used to design self-healing SMP based sealant, particularly for 1W-SMP based sealant. The reason is that compression programming is required for 1W-SMP sealant, and the joint reservoir provides the required external constraint during the healing process, making crack closure and healing feasible.

Disclosure statement

No potential conflict of interest was reported by the author(s).

Funding

This work was supported by National Science Foundation [grant number 1758674].

References

Al-Mansour, A. I., Sinha, K. C., & Kuczek, T. (1994). Effects of routine maintenance on flexible pavement condition. *Journal of Transportation Engineering*, *120*(1), 65–73. https://doi.org/10.1061/(ASCE)0733-947X(1994)120:1(65)

Al-Qadi, I., Dessouky, S., & Yang, S.-H. (2010). Linear viscoelastic modeling for hot-poured crack sealants at low temperature. *Journal of Materials in Civil Engineering*, *22*(10), 996–1004. https://doi.org/10.1061/(ASCE)MT.1943-5533.0000101

Al-Qadi, I., & Fini, E. (2011). Development of a crack sealant adhesion test (CSADT) specification for hot-poured bituminous sealants. *Journal of Testing and Evaluation*, *39*(2), 184–190. https://doi.org/10.1520/JTE103108

Al-Qadi, I., Fini, E., Elseifi, M., Masson, J., & McGhee, K. (2007a). Development of a viscosity specification for Hot-poured bituminous sealants. *Journal of Testing and Evaluation*, *35*(4), 395–403. https://doi.org/10.1520/JTE100260

Al-Qadi, I. L., Loulizi, A., Aref, S., Masson, J. F., & McGhee, K. M. (2005). Modification of bending beam rheometer specimen for low-temperature evaluation of bituminous crack sealants. *Transportation Research Record: Journal of the Transportation Research Board*, *1933*(1), 96–106. https://doi.org/10.1177/0361198105193300111

Al-Qadi, I., Yang, S.-H., Dessouky, S., & Masson, J. F. (2007b). Low-temperature characterization of hot-poured crack sealant by crack sealant direct tensile tester. *Transportation Research Record: Journal of the Transportation Research Board*, *1991*(1), 109–118. https://doi.org/10.3141/1991-13

Bag, M., Banerjee, S., Faust, R., & Venkataraman, D. (2016). Self-healing polymer sealant for encapsulating flexible solar cells. *Solar Energy Materials and Solar Cells*, *145*, 418–422. https://doi.org/10.1016/j.solmat.2015.11.004

Banerjee, S., Tripathy, R., Cozzens, D., Nagy, T., Keki, S., Zsuga, M., Faust, R., & Smart, P. (2015). Photoinduced smart, self-healing polymer sealant for photovoltaics. *ACS Applied Materials & Interfaces*, *7*(3), 2064–2072. https://doi.org/10.1021/am508096c

Behl, M., & Lendlein, A. (2007). Shape-memory polymers. *Materials Today*, *10*(4), 20–28. https://doi.org/10.1016/S1369-7021(07)70047-0

Biel, T. D., & Lee, H. (1997). Performance study of Portland cement concrete pavement joint sealants. *Journal of Transportation Engineering*, *123*(5), 398–404. https://doi.org/10.1061/(ASCE)0733-947X(1997)123:5(398)

Bommarito, T., Sparling, D. W., & Halbrook, R. S. (2010a). Toxicity of coal-tar pavement sealants and ultraviolet radiation to ambystoma maculatum. *Ecotoxicology*, *19*(6), 1147–1156. https://doi.org/10.1007/s10646-010-0498-8

Bommarito, T., Sparling, D. W., & Halbrook, R. S. (2010b). Toxicity of coal–tar and asphalt sealants to eastern newts, notophthalmus viridescens. *Chemosphere*, *81*(2), 187–193. https://doi.org/10.1016/j.chemosphere.2010.06.058

Britton, H. B. (1965). Bridge joint sealing – its materials and mechanical problems. *Highway Research Record 80 joints and sealants a symposium and other papers*.

Bryer, P. J., Scoggins, M., & McClintock, N. L. (2010). Coal-tar based pavement sealant toxicity to freshwater macroinvertebrates. *Environmental Pollution*, *158*(5), 1932–1937. https://doi.org/10.1016/j.envpol.2009.10.038

Bueno, M., Arraigada, M., & Partl, M. N. (2020). Induction heating technology for improving compaction of asphalt joints. *International Journal of Pavement Engineering*, *21*(12), 1532–1540. https://doi.org/10.1080/10298436.2018.1554218

Cao, L., Yang, C., Dong, Z., & Nonde, L. (2019). Evaluation of crack sealant adhesion properties under complex service ambient conditions based on the weak boundary layer (WBL) theory. *Construction and Building Materials*, *200*, 293–300. https://doi.org/10.1016/j.conbuildmat.2018.12.159

Carbonell-Blasco, P., Martín-Martínez, J. M., & Antoniac, I. V. (2013). Synthesis and characterization of polyurethane sealants containing rosin intended for sealing defect in annulus for disc regeneration. *International Journal of Adhesion and Adhesives*, *42*, 11–20. https://doi.org/10.1016/j.ijadhadh.2012.11.011

Chen, T., Qiu, J., Zhu, K., & Li, J. (2016). Electro-mechanical performance of polyurethane dielectric elastomer flexible micro-actuator composite modified with titanium dioxide-graphene hybrid fillers. *Materials & Design*, *90*, 1069–1076. https://doi.org/10.1016/j.matdes.2015.11.068

Chong, G. J. (1990). Rout and seal of cracks in flexible pavement: A cost-effective preventive maintenance procedure. *Transp. Res. Rec*, *1268*, 8–16.

Christen, K., Thacker, P. D., Schipper, O., & Renner, R. (2005). Scrutinizing pavement sealants for PAHs. *Environmental Science & Technology*, *39*(15), 312A–317A. https://doi.org/10.1021/es053317d

Clark, L. J., & Cosman, M. A. (2003). Use of permapol® P3.1 polymers and epoxy resins in the formulation of aerospace sealants. *International Journal of Adhesion and Adhesives*, *23*(5), 343–348. https://doi.org/10.1016/S0143-7496(03)00002-2

Eaton, R., & Ashcraft, J. (1992). State-of-the-Art Survey of Flexible Pavement Crack Sealing Procedures in the United States. *Rep. 91-18*, 24.

Evers, R. C.; Ontario Ministry of T. Communications Engineering Materials O. 1983. Evaluation of crack sealing compounds for asphaltic pavements: interim report no. 3. Engineering Materials Office, Ministry of Transportation and Communications.

Fan, J., & Li, G. (2017). High performance and tunable artificial muscle based on two-way shape memory polymer. *RSC Advances*, *7*(2), 1127–1136. https://doi.org/10.1039/C6RA25024F

Fan, J., & Li, G. (2018). High enthalpy storage thermoset network with giant stress and energy output in rubbery state. *Nature Communications*, *9*(1), 642–642. https://doi.org/10.1038/s41467-018-03094-2

Feng, X., Fan, J., Li, A., & Li, G. (2019). Multireusable thermoset with anomalous flame-triggered shape memory effect. *ACS Applied Materials & Interfaces*, *11*(17), 16075–16086. https://doi.org/10.1021/acsami.9b03092

Feng, X., & Li, G. (2020). Versatile phosphate diester-based flame retardant vitrimers via catalyst-free mixed transesterification. *ACS Applied Materials & Interfaces*, *12*(51), 57486–57496. https://doi.org/10.1021/acsami.0c18852

Foster, V. R. (1987). Polymers in caulking and sealant materials. *Journal of Chemical Education*, *64*(10), 861–865. https://doi.org/10.1021/ed064p861

Fried, A., Malladi, H., & Castorena, C. (2019). Impact of crack sealant on pavement skid resistance. *Transportation Research Record: Journal of the Transportation Research Board*, *2673*(7), 362–370. https://doi.org/10.1177/0361198119849590

Guo, M., Tan, Y., Du, X., & Lv, Z. (2017). Study on the cohesion and adhesion of hot-poured crack sealants. *Frontiers of Structural and Civil Engineering*, *11*(3), 353–359. https://doi.org/10.1007/s11709-017-0400-3

Hager, M., Bode, S., Weber, C., & Schubert, U. (2015). Shape memory polymers: Past, present and future developments. *Progress in Polymer Science*, *49-50*, 3–33. https://doi.org/10.1016/j.progpolymsci.2015.04.002

Haghayegh, M., & Mir Mohamad Sadeghi, G. (2012). Synthesis of shape memory polyurethane/clay nanocomposites and analysis of shape memory, thermal, and mechanical properties. *Polymer Composites*, *33*(6), 843–849. https://doi.org/10.1002/pc.22191

Herabat, P., & Kerdput, N. (2006). Analysis of damage mechanism of reinforced concrete pavement joint sealant. *Transportation Research Record: Journal of the Transportation Research Board*, *1958*(1), 90–99. https://doi.org/10.1177/0361198106195800111

Hu, X., Zhou, F., Hu, S., & Scullion, T. (2011). A new laboratory evaluation method for the adhesive performance of crack sealants. *Journal of Testing and Evaluation*, *39*(2), 177–183. https://doi.org/10.1520/JTE102845

Hu, J., Zhu, Y., Huang, H., & Lu, J. (2012). Recent advances in shape–memory polymers: Structure, mechanism, functionality, modeling and applications. *Progress in Polymer Science*, *37*(12), 1720–1763. https://doi.org/10.1016/j.progpolymsci.2012.06.001

Huber, M. P., Kelch, S., & Berke, H. (2016). FTIR investigations on hydrolysis and condensation reactions of alkoxysilane terminated polymers for use in adhesives and sealants. *International Journal of Adhesion and Adhesives*, *64*, 153–162. https://doi.org/10.1016/j.ijadhadh.2015.10.014

Ioannides, A., Long, A., & Minkarah, I. (2004). Joint sealant and structural performance at the Ohio Route 50 test pavement. *Transportation Research Record: Journal of the Transportation Research Board*, *1866*(1), 28–35. https://doi.org/10.3141/1866-04

Jancar, J., Douglas, J. F., Starr, F. W., Kumar, S. K., Cassagnau, P., Lesser, A. J., Sternstein, S. S., & Buehler, M. J. (2010). Current issues in research on structure–property relationships in polymer nanocomposites. *Polymer*, *51*(15), 3321–3343. https://doi.org/10.1016/j.polymer.2010.04.074

John, M., & Li, G. (2010). Self-healing of sandwich structures with a grid stiffened shape memory polymer syntactic foam core. *Smart Materials and Structures*, *19*(7), 075013(1-12). https://doi.org/10.1088/0964-1726/19/7/075013

Kendall, B. R. F. (1982). Anaerobic polymers as high vacuum leak sealants. *Journal of Vacuum Science and Technology*, *20*(2), 248–249. https://doi.org/10.1116/1.571276

Kiliaris, P., Papaspyrides, C. D., & Pfaendner, R. (2009). Influence of accelerated aging on clay-reinforced polyamide 6. *Polymer Degradation and Stability*, *94*(3), 389–396. https://doi.org/10.1016/j.polymdegradstab.2008.11.016

Kubit, A., Wydrzynski, D., & Trzepiecinski, T. (2018). Refill friction stir spot welding of 7075-T6 aluminium alloy single-lap joints with polymer sealant interlayer. *Composite Structures*, *201*, 389–397. https://doi.org/10.1016/j.compstruct.2018.06.070

Lee, S. W., & Stoffels, S. M. (2003). Effects of excessive pavement joint opening and freezing on sealants. *Journal of Transportation Engineering*, *129*(4), 444–450. https://doi.org/10.1061/(ASCE)0733-947X(2003)129:4(444)

Lendlein, A., & Kelch, S. (2002). Shape-memory polymers. *Angewandte Chemie International Edition*, *41*(12), 2034–2057. https://doi.org/10.1002/1521-3773(20020617)41:12 < 2034::AID-ANIE2034 > 3.0.CO;2-M

Li, G. (2014). *Self-healing composites: Shape memory polymer based structures*. West Sussex, UK: John Wiley & Sons, Inc.

Li, G. (2020). Liquid sealant with thermally adaptive properties. US Patent No. 10,633,541 B2.

Li, Q., Crowley, R. W., Bloomquist, D. B., & Roque, R. (2012). The creep testing apparatus (CRETA): A new testing device for measuring the viscoelasticity of joint sealant. *Journal of Testing and Evaluation*, *40*(3), 387-394. https://doi.org/10.1520/JTE104431

Li, Q., Crowley, R. W., Bloomquist, D. B., & Roque, R. (2014b). Newly developed adhesive strength test for measuring the strength of sealant between joints of concrete pavement. *Journal of Materials in Civil Engineering*, *26*(12), 04014097. https://doi.org/10.1061/(ASCE)MT.1943-5533.0001020

Li, F., Du, Y., & Li, L. (2017b). Viscoelastic model and stress relaxation evaluation of pavement crack sealants at low temperature. *Journal of Materials in Civil Engineering*, *29*(9), 04017135. https://doi.org/10.1061/(ASCE)MT.1943-5533.0001982

Li, A., Fan, J., & Li, G. (2018). Recyclable thermoset shape memory polymers with high stress and energy output via facile UV-curing. *Journal of Materials Chemistry A*, *6*(24), 11479–11487. https://doi.org/10.1039/C8TA02644K

Li, F., Huang, S. C., Xu, J., & Qin, Y. C. (2009). Performance evaluation and technical requirement of sealant and filler in asphalt pavement., Journal of Traffic and Transportation Engineering, *9*, 7–11. (In Chinese).

Li, G., Ji, G., & Meng, H. (2015b). Shape memory polymer-based sealant for a compression sealed joint. *Journal of Materials in Civil Engineering*, *27*(6), 04014196. https://doi.org/10.1061/(ASCE)MT.1943-5533.0001150

Li, G., & John, M. (2008). A self-healing smart syntactic foam under multiple impacts. *Composites Science and Technology*, *68*(15-16), 3337–3343. https://doi.org/10.1016/j.compscitech.2008.09.009

Li, G., King, A., Xu, T., & Huang, X. (2013). Behavior of thermoset shape memory polymer-based syntactic foam sealant trained by hybrid two-stage programming. *Journal of Materials in Civil Engineering*, *25*(3), 393–402. https://doi.org/10.1061/(ASCE)MT.1943-5533.0000572

Li, F., Li, L., & Li, T. (2015a). Viscosity Evaluation index of Hot-applied sealant for asphalt pavement. *Transportation Research Record: Journal of the Transportation Research Board*, *2481*(1), 83–89. https://doi.org/10.3141/2481-11

Li, F., Li, T., & Shi, X. (2014a). Evaluation on high-temperature adhesion performance of hot-applied sealant for asphalt pavement. *Journal of Wuhan University of Technology-Mater. Sci. Ed*, *29*(6), 1237–1241. https://doi.org/10.1007/s11595-014-1074-5

Li, Y., & Mao, S. (1996). Study on the properties and application of epoxy resin/polyurethane semi-interpenetrating polymer networks. *Journal of Applied Polymer Science*, *61*(12), 2059–2063. https://doi.org/10.1002/(SICI)1097-4628(19960919)61:12 < 2059::AID-APP2 > 3.0.CO;2-9

Li, G., & Nettles, D. (2010). Thermomechanical characterization of a shape memory polymer based self-repairing syntactic foam. *Polymer*, *51*(3), 755–762. https://doi.org/10.1016/j.polymer.2009.12.002

Li, K., Peng, J., Zhang, M., Heng, J., Li, D., & Mu, C. (2015b). Comparative study of the effects of anatase and rutile titanium dioxide nanoparticles on the structure and properties of waterborne polyurethane. *Colloids and Surfaces A: Physicochemical and Engineering Aspects*, *470*, 92–99. https://doi.org/10.1016/j.colsurfa.2015.01.072

Li, B., Ren, X., Li, Y., Ma, W., & Li, H. (2017a). Evaluation and selection of sealants and fillers using principal component analysis for cracks in asphalt concrete pavements. *Journal of Wuhan University of Technology-Mater. Sci. Ed*, *32*(2), 408–412. https://doi.org/10.1007/s11595-017-1611-0

Li, G., & Uppu, N. (2010). Shape memory polymer based self-healing syntactic foam: 3-D confined thermomechanical characterization. *Composites Science and Technology*, *70*(9), 1419–1427. https://doi.org/10.1016/j.compscitech.2010.04.026

Li, G., & Wang, A. (2016). Cold, warm, and hot programming of shape memory polymers. *Journal of Polymer Science Part B: Polymer Physics*, *54*(14), 1319–1339. https://doi.org/10.1002/polb.24041

Li, G., & Xu, T. (2011a). Thermomechanical characterization of shape memory polymer-based self-healing syntactic foam sealant for expansion joints. *Journal of Transportation Engineering*, *137*(11), 805–814. https://doi.org/10.1061/(ASCE)TE.1943-5436.0000279

Li, G., & Xu, W. (2011b). Thermomechanical behavior of thermoset shape memory polymer programmed by cold-compression: Testing and constitutive modeling. *Journal of the Mechanics and Physics of Solids*, *59*(6), 1231–1250. https://doi.org/10.1016/j.jmps.2011.03.001

Linde, S., & Johansson, U. (1992). Thermo-oxidative degradation of polymer modified bitumen. In K. R. Wardlaw & S. Shuler (Eds.), (pp. 244–253). ASTM International.

Liu, S., Mo, L., Wang, K., Xie, Y., & Woldekidan, M. F. (2016). Preparation, microstructure and rheological properties of asphalt sealants for bridge expansion joints. *Construction and Building Materials*, *105*, 1–13. https://doi.org/10.1016/j.conbuildmat.2015.12.017

Liu, H., Wang, H., Zhuang, C., Liu, Y., & Yin, J. (2013). Preparation of EA/PU IPN grouting material and its performances research. *Zhongnan Daxue Xuebao (Ziran Kexue Ban)/Journal of Central South University (Science and Technology)*, *44(8)*, 3129–3136.

Lu, L., Cao, J., & Li, G. (2017a). A polycaprolactone-based syntactic foam with bidirectional reversible actuation. *Journal of Applied Polymer Science*, *134*(34), 45225(1-12). https://doi.org/10.1002/app.45225

Lu, L., Cao, J., & Li, G. (2018). Giant reversible elongation upon cooling and contraction upon heating for a crosslinked cis poly(1,4-butadiene) system at temperatures below zero celsius. *Scientific Reports*, *8*(1), 14233(1-9). https://doi.org/10.1038/s41598-018-32436-9

Lu, L., Fan, J., & Li, G. (2016). Intrinsic healable and recyclable thermoset epoxy based on shape memory effect and transesterification reaction. *Polymer*, *105*, 10–18. https://doi.org/10.1016/j.polymer.2016.10.013

Lu, L., & Li, G. (2016). One-way multishape-memory effect and tunable two-way shape memory effect of ionomer poly(ethylene-co-methacrylic acid). *ACS Applied Materials & Interfaces*, *8*(23), 14812–14823. https://doi.org/10.1021/acsami.6b04105

Lu, L., Pan, J., & Li, G. (2017b). Recyclable high-performance epoxy based on transesterification reaction. *Journal of Materials Chemistry A*, *5*(40), 21505–21513. https://doi.org/10.1039/C7TA06397K

Lynch, L. N., & Janssen, D. J. (1998). Pavement joint sealant specifications – past, present, and future. *Journal of Elastomers & Plastics*, *30*(2), 161–181. https://doi.org/10.1177/009524439803000205

Mahler, B. J., Metre, P. C. V., Crane, J. L., Watts, A. W., Scoggins, M., & Williams, E. S. (2012). Coal-Tar-Based pavement Sealcoat and PAHs: Implications for the environment, human health, and stormwater management. *Environmental Science & Technology*, *46*(6), 3039–3045. https://doi.org/10.1021/es203699x

Mahler, B. J., Van Metre, P. C., Bashara, T. J., Wilson, J. T., & Johns, D. A. (2005). Parking Lot sealcoat: An unrecognized source of urban polycyclic aromatic hydrocarbons. *Environmental Science & Technology*, *39*(15), 5560–5566. https://doi.org/10.1021/es0501565

Malla, R. B., Shaw, M. T., Shrestha, M. R., & Brijmohan, S. B. (2007). Development and Laboratory analysis of silicone foam sealant for bridge expansion joints. *Journal of Bridge Engineering*, *12*(4), 438–448. https://doi.org/10.1061/(ASCE)1084-0702(2007)12:4(438)

Malla, R. B., Shrestha, M. R., Shaw, M. T., Brijmohan, S. B., Aging, T., & Compression Recovery, C. (2011). Temperature aging, compression recovery, creep, and weathering of a foam silicone sealant for bridge expansion joints. *Journal of Materials in Civil Engineering*, *23*(3), 287–297. https://doi.org/10.1061/(ASCE)MT.1943-5533.0000166

Masson, J. F. (1997). Effective sealing of pavement cracks in cold urban environments. *National Research Council Canada. Institute for Research in Construction*.

Masson, J. F., Collins, P., & Légaré P -P. (1999). Performance of pavement crack sealants in cold urban conditions. *Canadian Journal of Civil Engineering*, *26*(4), 395–401. https://doi.org/10.1139/l99-003

Masson, J. F., Collins, P., & Lowery, M. (2005). Temperature control of hot-poured sealants during the sealing of pavement cracks. *Construction and Building Materials*, *19*(6), 423–429. https://doi.org/10.1016/j.conbuildmat.2004.09.001

Masson, J.-F., Collins, P., Margeson, J., & Polomark, G. (2002). Analysis of bituminous crack sealants by physicochemical methods: Relationship to field performance. *Transportation Research Record: Journal of the Transportation Research Board*, *1795*(1), 33–39. https://doi.org/10.3141/1795-04

Masson, J. F., Collins, P., Perraton, D., & Al-Qadi, I. (2007). Rapid assessment of the tracking resistance of bituminous crack sealants. *Canadian Journal of Civil Engineering*, *34*(1), 126–131. https://doi.org/10.1139/l06-120

Masson, J.-F., & Lacasse, M. A. (1999). Effect of hot-air lance on crack sealant adhesion. *Journal of Transportation Engineering*, *125*(4), 357–363. https://doi.org/10.1061/(ASCE)0733-947X(1999)125:4(357)

Masson, J.-F., Lauzier, C., Collins, P., & Lacasse, M. A. (1998). Sealant degradation during crack sealing of pavements. *Journal of Materials in Civil Engineering*, *10*(4), 250–255. https://doi.org/10.1061/(ASCE)0899-1561(1998)10:4(250)

Meng, Q., & Hu, J. (2009). A review of shape memory polymer composites and blends. *Composites Part A: Applied Science and Manufacturing*, *40*(11), 1661–1672. https://doi.org/10.1016/j.compositesa.2009.08.011

Menon, A. V., Madras, G., & Bose, S. (2019). The journey of self-healing and shape memory polyurethanes from bench to translational research. *Polymer Chemistry*, *10*(32), 4370–4388. https://doi.org/10.1039/C9PY00854C

Nji, J., & Li, G. (2010a). A biomimic shape memory polymer based self-healing particulate composite. *Polymer*, *51*(25), 6021–6029. https://doi.org/10.1016/j.polymer.2010.10.021

Nji, J., & Li, G. (2010b). A self-healing 3D woven fabric reinforced shape memory polymer composite for impact mitigation. *Smart Materials and Structures*, *19*(3), 035007(1-9). https://doi.org/10.1088/0964-1726/19/3/035007

Nji, J., & Li, G. (2012). Damage healing ability of a shape-memory-polymer-based particulate composite with small thermoplastic contents. *Smart Materials and Structures*, *21*(2), 025011(1-10). https://doi.org/10.1088/0964-1726/21/2/025011

Odum-Ewuakye, B., & Attoh-Okine, N. (2006). Sealing system selection for jointed concrete pavements – a review. *Construction and Building Materials*, *20*(8), 591–602. https://doi.org/10.1016/j.conbuildmat.2005.01.042

Ozer, H., Solanki, P., Yousefi, S., & Al-Qadi, I. (2014). Field validation of laboratory-predicted Low-temperature performance of hot-poured crack sealants. *Transportation Research Record: Journal of the Transportation Research Board*, *2431*(1), 57–66. https://doi.org/10.3141/2431-08

Ozer, H., Yousefi, S., Al-Qadi, I., & Elizalde-Castro, G. (2015). Field aging and development of aging model for Hot-poured crack sealants. *Transportation Research Record: Journal of the Transportation Research Board*, *2481*(1), 90–99. https://doi.org/10.3141/2481-12

Pavlowsky, R. T. (2013). Coal-tar pavement sealant use and polycyclic aromatic hydrocarbon contamination in urban stream sediments. *Physical Geography*, *34*(4-5), 392–415. https://doi.org/10.1080/02723646.2013.848393

Petersen D. R., Rogers, A. D., Lee-Sullivan, P., & Bremner, T. (1998). A method of fatigue testing of concrete highway joint sealants in shear. *Journal of Testing and Evaluation*, *26*(3), 234–239. https://doi.org/10.1520/JTE11996J

Peterson, D. E. (1982). Resealing joints and cracks in rigid and flexible pavements. *Synthesis Rep. 98. Nat. Cooperative Hwy. Res. Program*.

Rodriguez, E. D., Luo, X., & Mather, P. T. (2011). Linear/network poly(ϵ-caprolactone) blends exhibiting shape memory assisted self-healing (SMASH). *ACS Applied Materials & Interfaces*, *3*(2), 152–161. https://doi.org/10.1021/am101012c

Rogers, A., Lee-Sullivan, P., & Bremner, T. (1999b). Selecting Concrete Pavement Joint Sealants. II: Case study. *Journal of Materials in Civil Engineering*, *11*(4), 309–316. https://doi.org/10.1061/(ASCE)0899-1561(1999)11:4(309)

Rogers, A. D., Lee-Sullivan, P., & Bremner, T. W. (1999a). Selecting Concrete Pavement Joint Sealants. I: Proposed test protocol. *Journal of Materials in Civil Engineering*, *11*(4), 302–308. https://doi.org/10.1061/(ASCE)0899-1561(1999)11:4(302)

Rosendahl, P. L., Staudt, Y., Schneider, A. P., Schneider, J., & Becker, W. (2019). Nonlinear elastic finite fracture mechanics: Modeling mixed-mode crack nucleation in structural glazing silicone sealants. *Materials & Design*, *182*, 108057(1-16). https://doi.org/10.1016/j.matdes.2019.108057

Ryu, S.W., Lin, W., & Cho, Y.-H. (2018). Experimental and numerical evaluations on the shape factor of silicone sealant for concrete pavements under vertical loading. *Journal of Performance of Constructed Facilities*, *32*(4), 04018032. https://doi.org/10.1061/(ASCE)CF.1943-5509.0001167

Sawalha, M., Ozer, H., Al-Qadi, I. L., & Xue, H. (2017). Development of a modified adhesion test for Hot-poured asphalt crack sealants. *Transportation Research Record: Journal of the Transportation Research Board*, *2612*(1), 85–95. https://doi.org/10.3141/2612-10

Scoggins, M., McClintock, N. L., Gosselink, L., & Bryer, P. (2007). Occurrence of polycyclic aromatic hydrocarbons below coal-tar-sealed parking lots and effects on stream benthic macroinvertebrate communities. *Journal of the North American Benthological Society*, *26*(4), 694–707. https://doi.org/10.1899/06-109.1

Shen, D., Shi, S., & Xu, T. (2018a). Synthesis and performance Evaluation of epoxy resin–modified shape memory polyurethane sealant. *Journal of Testing and Evaluation*, *46*(4), 1452–1461. https://doi.org/10.1520/JTE20170298

Shen, D., Shi, S., Xu, T., Huang, X., Liao, G., & Chen, J. (2018b). Development of shape memory polyurethane based sealant for concrete pavement. *Construction and Building Materials*, *174*, 474–483. https://doi.org/10.1016/j.conbuildmat.2018.04.154

Smith, K. L., & Romine, A. R. (1993). Innovative materials development and testing. volume 3: treatment of cracks in asphalt concretesurfaced pavements. *Rep. SHRP-H-354*.

Soliman, H., & Shalaby, A. (2009). Characterizing the low-temperature performance of hot-pour bituminous sealants using glass transition temperature and dynamic stiffness modulus. *Journal of Materials in Civil Engineering*, *21*(11), 688–693. https://doi.org/10.1061/(ASCE)0899-1561(2009)21:11(688)

Soliman, H., Shalaby, A., & Eng, P. Evaluation of Joint and Crack Sealants Based on Cyclic Loading and Rheological Properties. 2007 *Annual Conference of the Transportation Association of Canada* 2007.

Soliman, H., Shalaby, A., & Kavanagh, L. (2008). Performance evaluation of joint and crack sealants in cold climates using DSR and BBR tests. *Journal of Materials in Civil Engineering*, *20*(7), 470–477. https://doi.org/10.1061/(ASCE)0899-1561(2008)20:7(470)

Stögbauer, H., & Wolf, A. T. (1991). The influence of heat ageing on one-part construction silicone sealants. *Construction and Building Materials*, *5*(1), 27–32. https://doi.org/10.1016/0950-0618(91)90029-K

Tan, X. Y., Zhang, J. P., Guo, D., Sun, G. Q., Zhou, Y. Y., Zhang, W. W., & Guan, Y. S. (2020). Preparation, characterization and repeated repair ability evaluation of asphalt-based crack sealant containing microencapsulated epoxy resin and curing agent. *Construction and Building Materials*, *256*, 119433(1-13). https://doi.org/10.1016/j.conbuildmat.2020.119433

Thakur, S., & Karak, N. (2015). Tuning of sunlight-induced self-cleaning and self-healing attributes of an elastomeric nanocomposite by judicious compositional variation of the TiO2–reduced graphene oxide nanohybrid. *Journal of Materials Chemistry A*, *3*(23), 12334–12342. https://doi.org/10.1039/C5TA02162F

Tock, R. W., Chew, C. H., & Minor, J. E. (1987). Determination of the modulus of elasticity of structural silicone sealants. *TTU-IDR-84D, National Science Foundation*. http://hdl.handle.net/2346/61585.

Van Metre, P. C., & Mahler, B. J. (2014). PAH concentrations in lake sediment decline following ban on coal-Tar-based pavement sealants in Austin, texas. *Environmental Science & Technology*, *48*(13), 7222–7228. https://doi.org/10.1021/es405691q

Van Metre, P. C., Majewski, M. S., Mahler, B. J., Foreman, W. T., Braun, C. L., Wilson, J. T., & Burbank, T. L. (2012). PAH volatilization following application of coal-tar-based pavement sealant. *Atmospheric Environment*, *51*, 108–115. https://doi.org/10.1016/j.atmosenv.2012.01.036

Ward, D. R. (1993). Evaluation of crack sealant performance on indiana's asphalt concrete surfaced pavements. *Indiana Dept. of Transp., Ind*.

Why Sealant Joints Fail: Avoiding Sealant Application Failures. (2018). https://vinats.com/en/why-sealant-joints-fail-avoiding-sealant-application-failures/

Wick, C. D., Peters, A. J., & Li, G. (2021). Quantifying the contributions of energy storage in a thermoset shape memory polymer with high stress recovery: A molecular dynamics study. *Polymer*, *213*, 123319. https://doi.org/10.1016/j.polymer.2020.123319

Wilde, W. J., & Johnson, E. N. (2009). Effect of crack sealant material and reservoir geometry on surface roughness of bituminous overlays. *Transportation Research Record: Journal of the Transportation Research Board*, *2108*(1), 69–74. https://doi.org/10.3141/2108-08

Williams, E. S., Mahler, B., & Van Metre, P. C. (2012). Coal-tar pavement sealants might substantially increase children's PAH exposures. *Environmental Pollution*, *164*, 40–41. https://doi.org/10.1016/j.envpol.2012.01.010

Williams, E. S., Mahler, B. J., & Van Metre, P. C. (2013). Cancer risk from incidental ingestion exposures to PAHs associated with coal-tar-sealed pavement. *Environmental Science & Technology*, *47*(2), 1101–1109. https://doi.org/10.1021/es303371t

Wu, H., Zhu, M., Liu, Z., & Yin, J. (2015). Developing a polymer-based crack repairing material using interpenetrate polymer network (IPN) technology. *Construction and Building Materials*, *84*, 192–200. https://doi.org/10.1016/j.conbuildmat.2015.03.067

Xu, T., & Li, G. (2011a). Cyclic stress-strain behavior of shape memory polymer based syntactic foam programmed by 2-D stress condition. *Polymer*, *52*(20), 4571–4580. https://doi.org/10.1016/j.polymer.2011.08.005

Xu, T., & Li, G. (2011b). Durability of shape memory polymer based syntactic foam under accelerated hydrolytic ageing. *Materials Science and Engineering: A*, *528*(24), 7444–7450. https://doi.org/10.1016/j.msea.2011.06.055

Xu, T., Li, G., & Pang, S.-S. (2011b). Effects of ultraviolet radiation on morphology and thermo-mechanical properties of shape memory polymer based syntactic foam. *Composites Part A: Applied Science and Manufacturing*, *42*(10), 1525–1533. https://doi.org/10.1016/j.compositesa.2011.07.005

Xu, L., Shang, P., Xu, X. W., Herrick, A. M., Sgro, A., & Shou, C. Q. (2011a). Studies on synthesis and properties of novel polyurethane pavement joint sealant modified with polydimethysiloxane. *Materials Research Innovations*, *15*(2), 150–155. https://doi.org/10.1179/143307511X12998222919119

Xue, H., Cao, L., Hou, X., & Tan, Y. (2018). Cohesive property evaluation of crack sealants using a low-temperature tensile tester. *Journal of Testing and Evaluation*, *46*(5), 1983–1994. https://doi.org/10.1520/JTE20160319.

Yan, C., & Li, G. (2020). A mechanism-based four-chain constitutive model for enthalpy-driven thermoset shape memory polymers with finite deformation. *Journal of Applied Mechanics*, *87*(6), 061007(1-10). https://doi.org/10.1115/1.4046583

Yan, C., Yang, Q., & Li, G. (2020). A phenomenological constitutive model for semicrystalline two-way shape memory polymers. *International Journal of Mechanical Sciences*, *177*(105552), 1–14. https://doi.org/10.1016/j.ijmecsci.2020.105552

Yang, S.-H., Al-Qadi, I., McGraw, J., Masson, J. F., & McGhee, K. (2010). Threshold identification and Field Validation of performance-based guidelines to select Hot-poured crack sealants. *Transportation Research Record: Journal of the Transportation Research Board*, *2150*(1), 87–95. https://doi.org/10.3141/2150-11

Yang, Q., Fan, J., & Li, G. (2016). Artificial muscles made of chiral two-way shape memory polymer fibers. *Applied Physics Letters*, *109*(183701), 1–5. https://doi.org/10.1063/1.4966231

Yang, Q., & Li, G. (2016). A top-down multi-scale modeling for actuation response of polymeric artificial muscles. *Journal of the Mechanics and Physics of Solids*, *92*, 237–259. https://doi.org/10.1016/j.jmps.2016.04.007

Yin, J., Pang, Q., Wu, H., & Song, W. (2018). Using a polymer-based sealant material to make crack repair of asphalt pavement. *Journal of Testing and Evaluation*, *46*(5), 2056–2066. https://doi.org/10.1520/JTE20170041

Yun, T., Lee, O., Lee, S. W., Kim, I. T., & Cho, Y. H. (2011). A performance evaluation method of preformed joint sealant: Slip-down failure. *Construction and Building Materials*, *25*(4), 1677–1684. https://doi.org/10.1016/j.conbuildmat.2010.10.015

Zhang, Y., & Hourston, D. J. (1998). Rigid interpenetrating polymer network foams prepared from a rosin-based polyurethane and an epoxy resin. *Journal of Applied Polymer Science*, *69*(2), 271–281. https://doi.org/10.1002/(SICI)1097-4628(19980711)69:2 < 271::AID-APP8 > 3.0.CO;2-K

Zhang, J., Manias, E., Polizos, G., Huh, J.-Y., Ophir, A., Songtipya, P., Del, M., & Jimenez-Gasco, M. D. M. (2009). Tailored polyethylene nanocomposite sealants: Broad-range peelable heat-seals through designed filler/polymer interfaces. *Journal of Adhesion Science and Technology*, *23*(5), 709–737. https://doi.org/10.1163/156856108X379182

Zhang, P., Ogunmekan, B., Ibekwe, S., Jerro, D., Pang, S.-S., & Li, G. (2016). Healing of shape memory polyurethane fiber-reinforced syntactic foam subjected to tensile stress. *Journal of Intelligent Material Systems and Structures*, *27*(13), 1792–1801. https://doi.org/10.1177/1045389X15610912

Zimmer, T., Carpenter, S., & Darter, M. (1984). Field performance of a low-modulus silicone highway joint sealant. *Transportation Research Record*, *990*, 31–37. http://worldcat.org/isbn/0309037743

Zohrevand, A., Ajji, A., & Mighri, F. (2014). Morphology and properties of highly filled iPP/TiO2 nanocomposites. *Polymer Engineering & Science*, *54*(4), 874–886. https://doi.org/10.1002/pen.23625.